# IMPACT OF PROCESS PARAMETER MODIFICATION ON POLY(3-HEXYLTHIOPHENE) FILM MORPHOLOGY AND CHARGE TRANSPORT

A Thesis
Presented to
The Academic Faculty

by

Jiho Lee

In Partial Fulfillment
of the Requirements for the Degree
Masters of Science in the
School of Chemical and Biomolecular Engineering

Georgia Institute of Technology
December 2013

# IMPACT OF PROCESS PARAMETER MODIFICATION ON POLY(3-HEXYLTHIOPHENE) FILM MORPHOLOGY AND CHARGE TRANSPORT

Approved by:


Dr. Elsa Reichmanis, Advisor
School of Chemical and Biomolecular Engineering
*Georgia Institute of Technology*

Dr. William J. Koros
School of Chemical and Biomolecular Engineering
*Georgia Institute of Technology*

Dr. Dennis W. Hess
School of Chemical and Biomolecular Engineering
*Georgia Institute of Technology*

Dr. Yulin Deng
School of Chemical and Biomolecular Engineering
*Georgia Institute of Technology*


Date Approved: November 13, 2013

# ACKNOWLEDGEMENTS

I would like to make special thanks to my advisor Elsa Reichmanis who gave me remarkable opportunities by allowing research in the group. I will remember her as a person with deep patience and understanding. Her optimism and support were great cheers to me. Also I share thanks to my committee, Prof. Dennis Hess, William Koros, and Yulin Deng, whom I am very proud to be associated with. I will remember Professor Hess who provided me an advice in making decisions for my future. With his help, I decided to further pursue research in graduate school. Professor Koros and Deng were very generous and responded without any feeling of troublesome to my irregular requests.

Many thanks and best wishes to all of our Reichmanis' research group members, without your support, the research may have been impossible to start. Especially, Mincheol Chang, have been a direct mentor to me. He taught me necessary concepts to be successful in my career. The hard-work we had in the laboratory will be remembered as rewarding memories. Thank you Dalsu Choi, Boyi Fu, Ping-Hsun Chu, Nabil Kleinhenz, Ji-Hwan Kang, Jeff Hernandez, and Ashwin for your support in this group. It has been a pleasure sharing and working together with all of you.

Most importantly, I thank my God, Jesus Christ who owns and shepherds my life. In every moment, I believe that my life is and will be in God's hands. I wish to thank my family and friends, with their encouragement and support I managed to joyfully finish this study. I am very proud to be a community of Student For Christ (SFC) and Imitators of Christ Church Atlanta (ICCA). I cannot speak of my Georgia Tech life without mentioning them. I share great appreciations to you all for your love and memories.

# TABLE OF CONTENTS

# LIST OF TABLES

# LIST OF FIGURES

Page

## SUMMARY

Organic electronics based on π-conjugated semi-conductor raises new technology, such as organic film transistors, e-paper, and organic photovoltaic cells that can be implemented cost-effectively on large-area applications. Currently, the device performance is limited by low charge carrier mobility. Poly(3-hexylthiophene) (P3HT) and organic field effect transistors (OFET) is used as a model to investigate morphology of the organic film and corresponding electronic properties. In this thesis, processing parameters such as boiling points and solubility are controlled to impact the micro- and macro-morphology of the film to enhance the charge transport of the device.

Alternative approach to improve ordering of polymer chains and increase in charge transport without post-treatment of P3HT solution is studied. The addition of high boiling good solvent to the relatively low boiling main solvent forms ordered packing of π-conjugated polymers during the deposition process. We show that addition of 1% of dichlorobenzene (DCB) to the chloroform based P3HT solution was sufficient to improve wetting and molecular structures of the film to increase carrier mobility.

Systematic study of solvent-assisted re-annealing technique, which has potential application in OFET encapsulation and fabrication of top-contact OFET, is conducted to improve mobility of OFET, and, to suggest a cost-effective processing condition suitable for industrial application. Three process parameters: boiling point, polarity, and solubility are investigated to further understand the trend of film response to the solvent-assisted technique. We report the high boiling non-polar solvents with relatively high RED values promote highest improvement in molecular packing and formulate crystalline structure of the thin film, which increases the device performance.

# CHAPTER 1

# INTRODUCTION

Electronic devices have greatly enhanced the quality of our lives and have become essential components of our daily activity. Recent development of the 'smart-phone' has allowed people to conveniently access daily news, games, and even perform banking through a few touches on the screen. This device is a result of microelectronics, which utilizes miniaturized design and components to manufacture electronics such as transistors, resistors, and capacitors. These miniaturized electronics elements can be integrated together into large-scale devices and circuits forming macroelectronics. For example, multiple light - emitting diodes (LED) together can represent multiple pixels to construct a flat-screen display. Not only is macroelectronics associated with commercial industries, it can be applied to the emerging technology of organic electronics, which offers the possibility for printing of circuits on flexible substrates and for the development of mass production system of devices by using fabrication methods such as ink-jet printing.[1-2] The primary operation of organic electronics is replacement of silicon with conductive polymers. Conductive polymers, although the subject of many investigations, are yet to catch up in performance with silicon alternatives. Hence, the main objective of organic electronics is not to replace silicon but discover technologies that utilize the unique capabilities of organics or the combination of both materials. Typical applications of organic electronics are e-paper, organic light emitting diodes (OLEDs), organic solar cells, and organic field effect transistors (OFETs) (Figure 1). In this thesis, OFET will be investigated to study the performance of the organic films processed under different conditions.

(a) (b) (c)

**Figure 1-** Example applications of organic electronics. (a) organic solar cell[3], (b) OFET based display[4], (c) e-paper[5].

## 1.1 Organic Electronics

Unlike the rigid and crystalline structure of inorganic electronics materials, organic polymers can be printed on a flexible substrate due to their ability to be processed at a relatively lower temperature than inorganic counterparts. Organic materials can be processed in a solvent that allows large area fabrication of electronic device structures, which consequently reduces the cost of production. Due to this printability, organic electronics are sometimes referred to as printed electronics. The comparison between organic electronics and conventional inorganic electronics is shown in Figure 2.

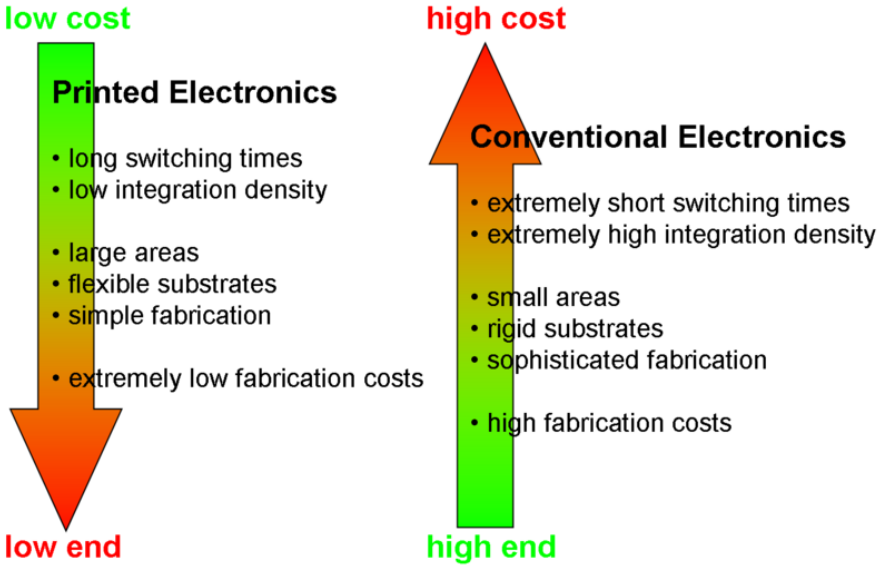


**Figure 2-**Comparison between organic and conventional silicon electronics[6]

In the late 20th century, anthracene[7] and polyacetylene[8] were among the earlier materials discoveries in the field of organic electronics. However, the early forms of the synthesized compounds were not yet practical for technology applications.[9] After about 10 years of constant research, the field expanded with the discovery of organic materials that demonstrated electrical properties similar to metals. One of them relates to the discovery of π-conjugated polymers, which exhibit conductive properties. Detailed properties and mechanisms associated with π-conjugated polymers will be dealt in the following section.

## 1.2 Charge transport in π-conjugated polymers

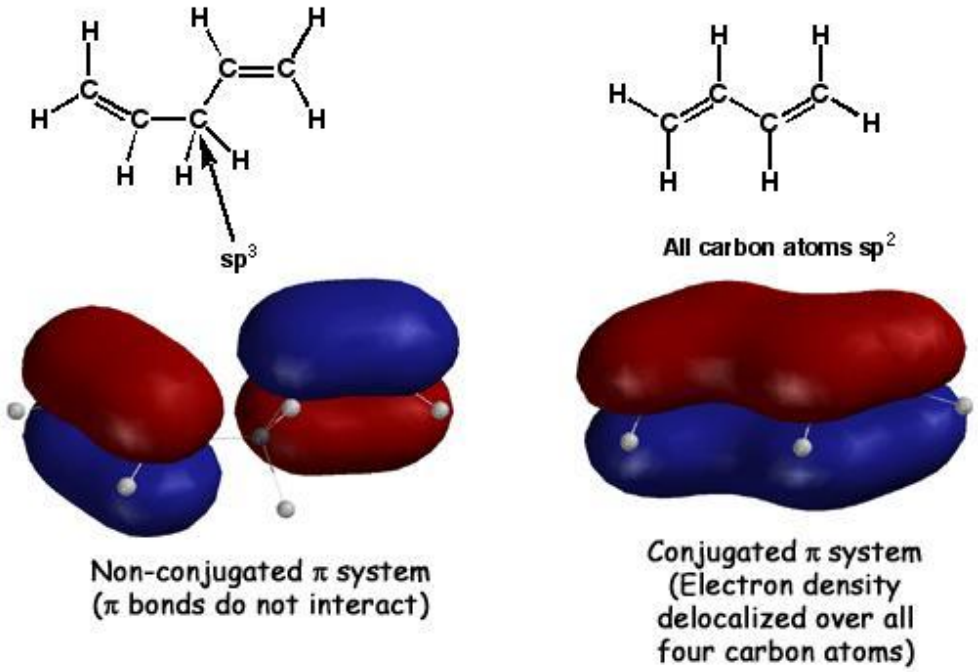


**Figure 3**-Comparison between non-conjugated and conjugated π system[10]

Polymers known as π-conjugated polymers contain a π-conjugated system, which refers to a series of carbon atoms covalently bonded with alternating single and double bonds. These π-conjugated carbons are structured in a $sp^2 + p_z$ manner, where the $p_z$-orbital is orthogonal to the $sp^2$ carbon atoms. The π-electrons present in the p-orbitals are

delocalized meaning that they can navigate along the main backbone of the polymer. The π-conjugated polymers gain conductivity through this delocalization of electrons. The importance of conjugation is shown in Figure 3 above. Even though p-orbitals are present in the 1, 3-pentadiene the π-bonds are disconnected with a single $sp^3$ bond, preventing charge transfer. On the other hand, butadiene, a conjugated system, constructs a "π-road" for charge carriers to move along the backbone of the chain.

Introducing π-orbital to sigma ($\sigma$) bonds greatly influences the structure of the molecule. Strong coupling of electrons induced by π-electron densities alters the geometry of the molecule, which is shown in Figure 4 with an example of butadiene.

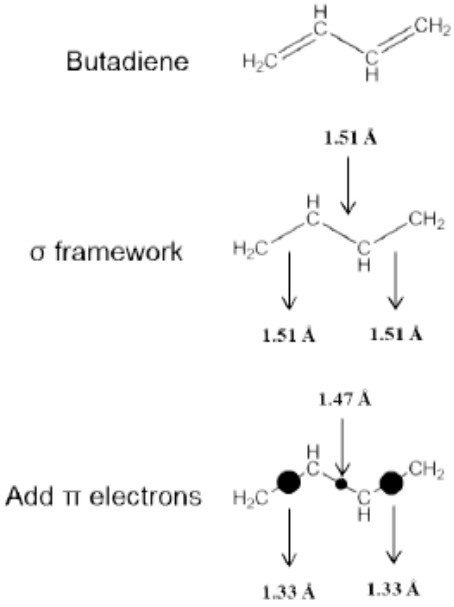


**Figure 4 -** Geometrical structure of butadiene with and without introduction of π-electrons. Black circles indicate π-electron densities. Obtained from[11].

With this strong coupling, electrons interact with phonons in both ground and excited states to form polarons.[12] Polaron refers to a quasi-particle that originates when charge carriers are introduced into conjugated systems. Due to the strong cloud of polarization surrounding the charged particle, the lattice geometry of the system constantly adjusts to moving charges. These polarons provide a good explanation of the charge carriers in organic semi-conductors that are held together with weak covalent

bonds and strong Van der Waals forces. Due to the weak lattice structure, a polaron induces deformation in the molecule's structure, which results in self-trapping of charge carriers.[13] Mechanism to "hop" this trapping will be outlined later. The image of a polaron in a central benzene atom is represented in Figure 5.

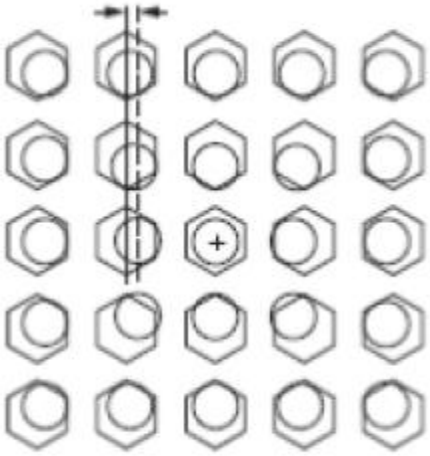

**Figure 5:** The polarization effect is outlined. Extra charge present in the benzene induces clouds of polarization. Image obtained from[12]

The presence of π-electrons in conjugated polymers is a key reason for charge transport due to delocalization and polarization. Charge transport in organic materials can quantitatively be compared with charge carrier mobility. When an electric field *E* is applied, electrons experience a generated external force. The average drift velocity or $< v_d >$ can be represented as Equation 1, where $t$ is collision time and $m_e$ is the effective mass of an electron.

$$< v_d >= -\frac{eEt}{m_e} \tag{1}$$

The ratio of this average drift velocity to the applied electric field is known as carrier mobility[14] ( $\mu$ ), in this derivation, it is electron mobility as shown in Equation 2. A hole mobility can be found by substituting an effective electron mass with an effective hole mass.

$$\mu = \frac{< v_d >}{E} = -\frac{et}{m_e} \tag{2}$$

The presence of disorder in the weakly bonded organic polymers traps charges. Hence, in the conjugated system, charge transfers by a hopping mechanism represented in Figure 6. Hopping is transfer of charge from an ionized molecule to a neutral molecule.

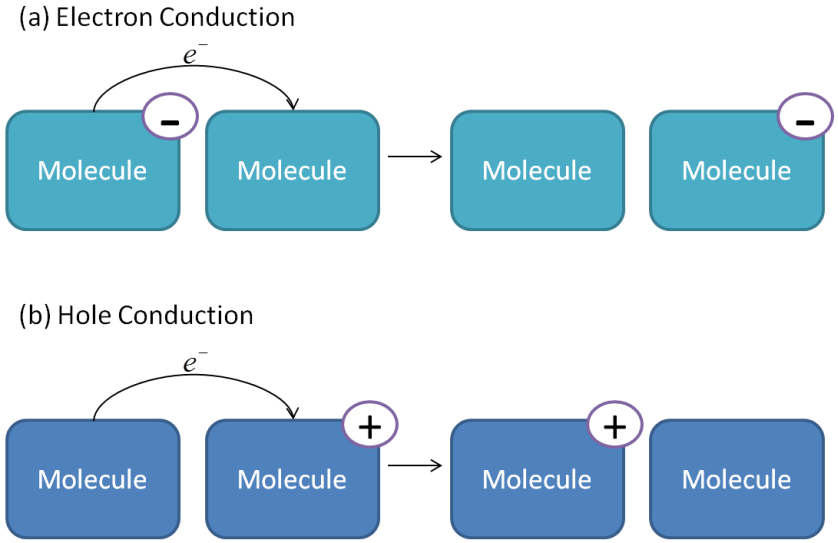


**Figure 6:** Charge hopping under the influence of electric field. (a) and (b) represent hole and electron conduction, respectively.

Charge hopping mechanism can be explained with Marcus electron transfer theory[15-16],which is shown in Equation 4, where $k_{hop}$ is the hopping rate of a charge carrier such as holes, $k_B$ is the Boltzmann constant, $T$ is the absolute temperature, $\hbar$ is reduced Planck's constant, $V$ is the electronic coupling between initial and final states, and $\lambda$ is the reorganization energy.

$$k_{hop} = \left(\frac{\pi}{\lambda k_B T}\right)^{\frac{1}{2}} \frac{V^2}{\hbar} \exp\left(-\frac{\lambda}{4k_B T}\right) \tag{4}$$

The geometry of a charged molecule is different from the geometry of a neutral molecule, hence as charges hop from ionized molecule to neutral molecule there is reorganization energy to change the geometry of the molecules. Therefore, charge

hopping is maximized with an increase in electronic coupling and with a decrease in reorganization energy.

Typically, disordered conjugated polymers exhibit much smaller carrier mobilities compared to inorganic materials, and are typically in the range of about $10^{-5}$-$10^{-1}\,cm^2V^{-1}s^{-1}$[17]. This is because many organic semi-conductors are structurally disordered and trap charge carriers preventing transfer. Therefore the morphology of the film greatly impacts mobility of the organic semi-conductor. Recently, conjugated polymers that form an amorphous film upon coating have been processed to exhibit mobilities in the range within $1\,cm^2V^{-1}s^{-1}$[18]. Within the same material, the order, or arrangement of the molecules may impact mobility, and depending on process conditions may differ by orders of magnitude.

## 1.3 Material: Poly(3-hexylthiophene)

Easily processable, and yet highly conductive organic materials, are an active area of research since the 20th century. Molecular semiconductors and polymeric semiconductors are the two main categories of conductive materials. Among these organic materials, polymeric semiconductors, also known as conjugated polymers, are highlighted for their unique mechanical and rheological properties that allow large-area processing and application.[19] A few examples of these organic materials are displayed in Figure 7.

Polythiophenes were one of the earlier forms of polymers that were used to study the mechanism of charge transport in organic semiconductors. However, polythiophenes were difficult to be processed in solution.[20] This obstacle was solved by Elsenbaumer et al, who incorporated alkyl side chains that afforded solubility to the insoluble thiophene backbone.[21] In this thesis specifically, poly(3-hexylthiophene) (P3HT) from the

poly(alkylthiophene) (PAT) group is used as a base material because of its solubility in a variety of solvents and good mobility.[22]

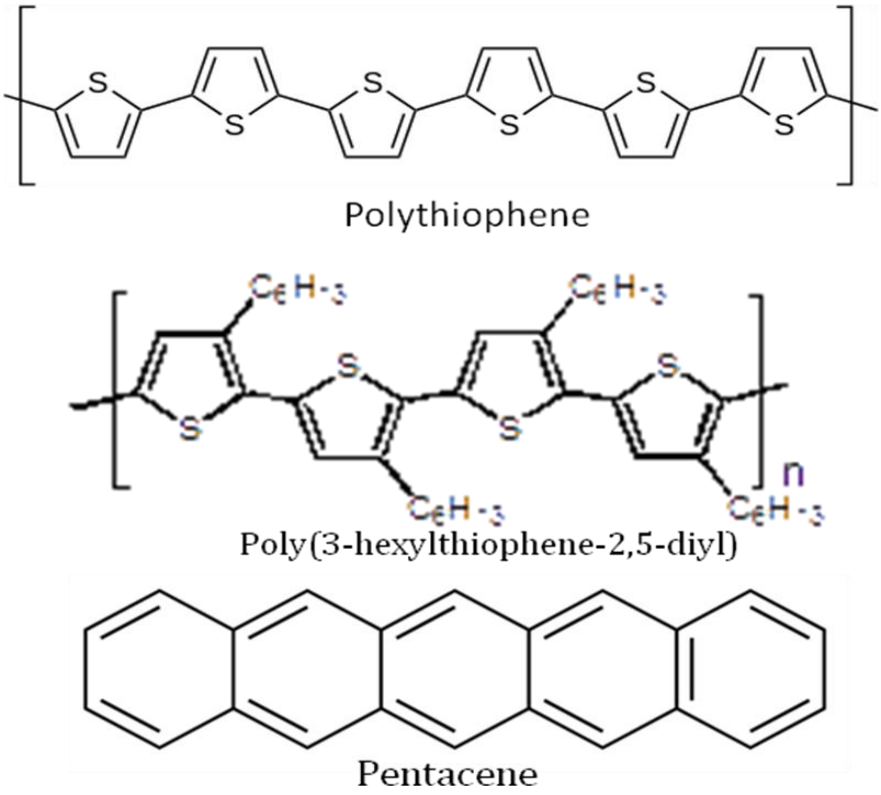


**Figure 7:** Representative organic polymers[23-24]

P3HT consists of the conjugated polythiophene backbone and hexyl side chains. The main backbone contributes the most to the charge transport direction, while the side chain solubilizes the polymer. Figure 8 shows how this P3HT can be ordered. Rapid charge transport occurs when P3HT is packed together the *c*-direction forming a long series of connected conjugated polymer backbones. Charge transport is also fast across the *b*-direction where π-π stacking occurs due to delocalization of electrons in the π-orbitals. Finally, charge can transfer through alkyl side chains towards the *a*-direction. However, the side chains act as a good insulator, hence, we can assume minimal charge transport in the *a*-direction. These side chains affect solubility of the polymer. When the alkyl chain is short, there will not be adequate solubility induced to the polymer. On the

other hand, when the side chain is too long, the alkyl groups hinder packing of P3HT and result in disorder in the P3HT packed structure.

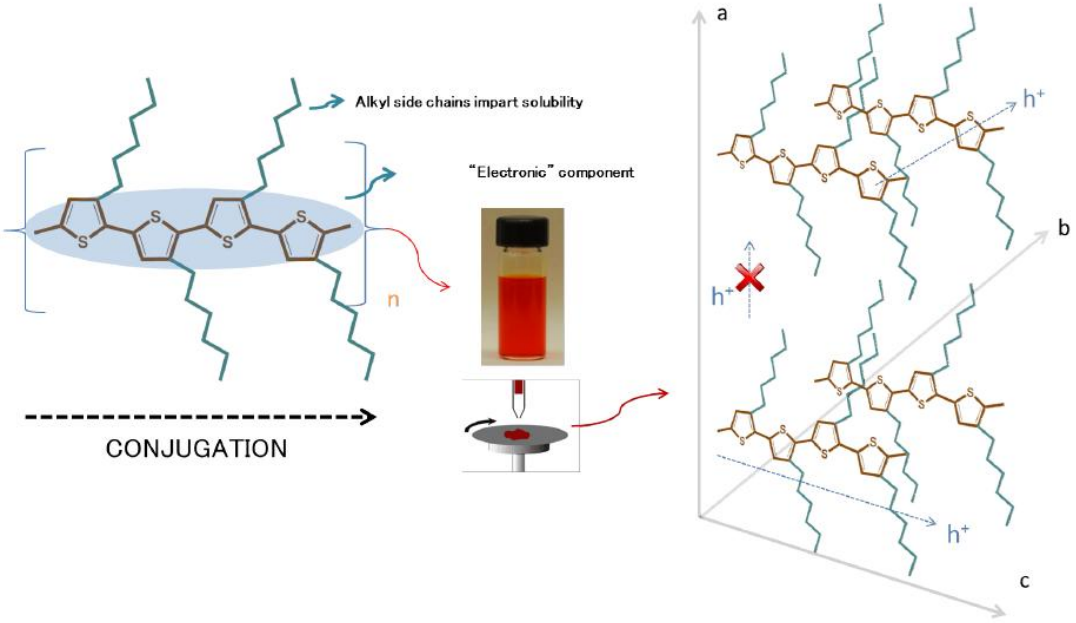


**Figure 8:** P3HT and its packing in Cartesian coordinate. Rapid charge transport takes place in the b- axis, which is pi-pi stacking direction and c-axis, which is main backbone direction. Image obtained from[25].

During P3HT film formation, a fiber-texture appears when π-orbitals stack in the out-of-plane direction (*b*-direction) relative to the substrate as shown in Figure 8. The device performance of P3HT is heavily affected by morphology and ordering of the film. Even though P3HT no longer exhibits the best mobility in OFETs, it is chosen for our investigation because it has been studied extensively in the literature. Based upon additional thorough studies on P3HT, we will be able to understand the mechanism behind the performance of OFET with defined changes in process parameters. In this thesis process parameters such as boiling point, polarity and solubility of solvents are controlled to investigate their impact on P3HT based OFET devices.

## 1.4 Organic Field Effect Transistor (OFET) Devices

The first organic field effect transistor (OFET) was fabricated by Tsumura et. al. in 1986 using a polythiophene film, which showed mobility of $10^{-5} cm^2V^{-1}s^{-1}$ [26]. The performance of OFETs has improved ever since to approximately 1 $cm^2V^{-1}s^{-1}$ [27]. Operation of an OFET is similar to a metal oxide semiconductor field effect transistor or MOSFET. By controlling gate voltage, current flowing between source and drain electrodes can be manipulated. Performance of an OFET (such as field effect mobility) can be calculated, and can provide a measure of the impact of film morphology on charge transport. In this thesis, OFETs have been fabricated and tested to study the impact of process parameters on device performance.

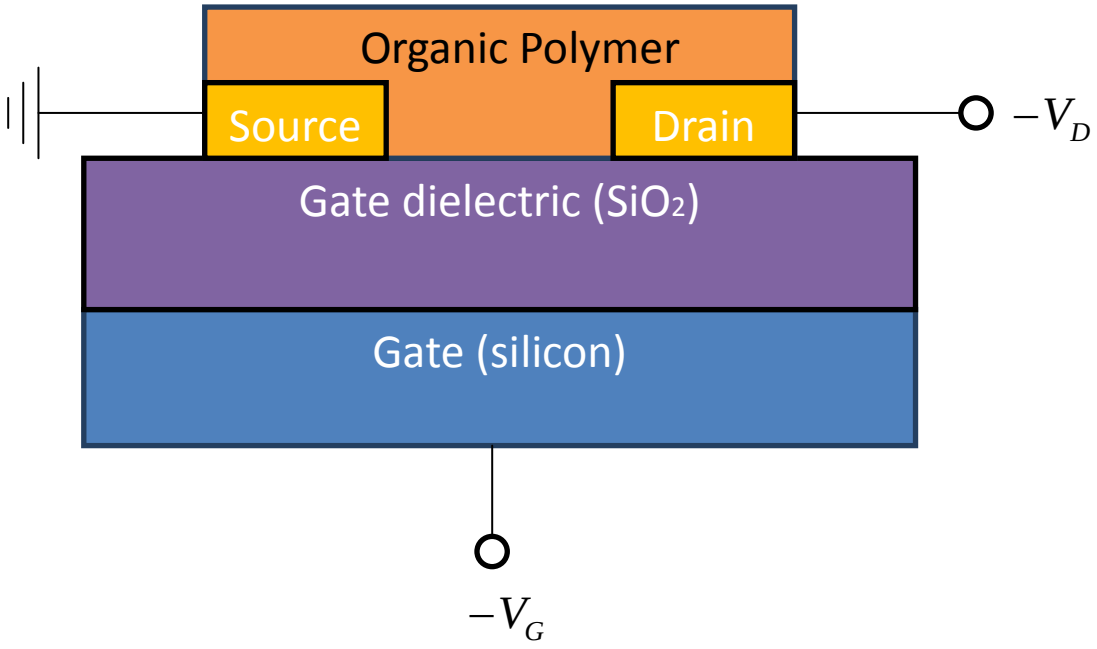


**Figure 9:** Geometry of Bottom-contact OFET. Source electrode is grounded. Drain and gate electrodes both have negative voltage.

An OFET mainly consists of a source, drain, and gate electrode that can be deposited in different kinds of geometries.[28] Silicon oxide, which acts as a gate dielectric separates direct contact between the two electrodes and the gate. Bottom-contact

fabrication method is suitable for large-area production, as well as, small scale transistor design. Moreover, this geometry was chosen in the thesis because of its convenience in fabrication. The bottom-contact configuration is represented in Figure 9.

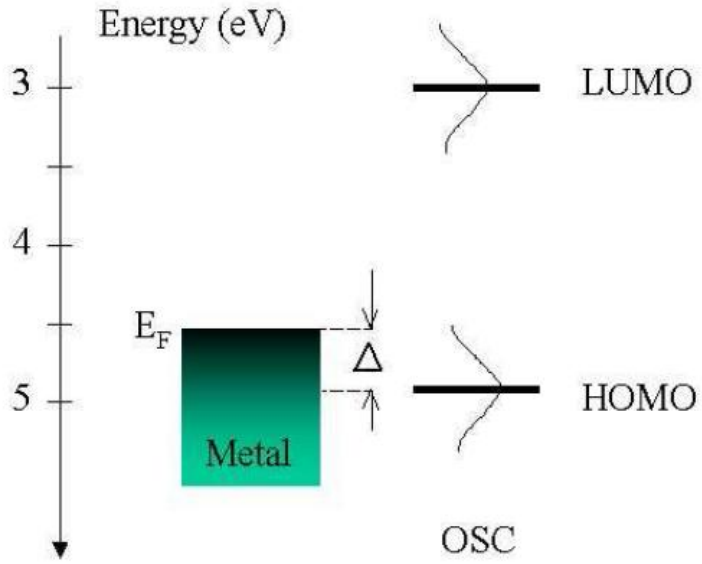


**Figure 10:** The energy diagram that shows the band alignment at polymer-metal interface such as petacene-gold interface. By overcoming an intrinsic energy barrier ( $\Delta$ ), holes in the Fermi level of the metal transfers to HOMO level of the organic semiconductor (OSC). Image obtained from[29].

FETs can operate in inversion and accumulation mode. MOSFETs operate in the inversion mode and OFETs operate in the accumulation mode. OFETs can either operate in p-channel or n-channel mode, which means charge carriers are either holes (positive charge carrier) or electrons, respectively. Even though technically, p-type and n-type devices should perform similarly, p-channel materials have been more extensively investigated because they generally display better charge transport properties. In a p-type OFET, when a negative gate voltage (e.g. $V_G$ = -80V) is applied, holes will be injected into the organic polymer layer if the hole injection barrier or intrinsic energy barrier ( $\Delta$ ) between the Fermi level of the gate dielectric (e.g. silicon oxide) and highest occupied

molecular orbital (HOMO) level of organic polymer (e.g. P3HT) is small as shown in Figure 10. The holes accumulate in the organic semiconductor (OSC) forming a conducting layer between the source and drain electrodes. Then the potential difference between source and drain electrodes ($V_D$-$V_S$) drives the charge transport through this pathway. Finally, the charges are collected as drain current.

By assuming the Shockley gradual channel approximation, we can characterize OFETs quantitatively. This approximation assumes that change in the channel width is very small compared to the width of the channel. That means the electric field normal to the conductive channel is much larger than the electric field along the channel. This Shockley approximation is applied to typical OFETs, which have a channel length much larger than the thickness of the semiconductor film.

OFETs can operate in the linear regime and the saturation regime (Equation 5 and 6). They are defined with several parameters: channel width between source and drain region ($W$), channel length between source and drain electrodes ($L$), capacitance of the gate dielectric ($C_{OX}$), mobility of charge carriers ($\mu$), drain, source, gate and threshold voltages ($V_D, V_S, V_G$, and $V_T$). Threshold voltage ($V_T$) is defined as voltage required to start the charge transport in the source and drain region.

$$I_{D,Linear} = \frac{W}{L}\mu C_{OX}(V_G - V_T)V_D \quad \text{for } V_D \le V_{Dsat} = V_G - V_T \tag{5}$$

$$I_{D,Sat} = \left(\frac{1}{2}\right)\frac{W}{L}\mu C_{OX}(V_G - V_T)^2 \quad \text{for } V_D \ge V_{Dsat} = V_G - V_T \tag{6}$$

In the linear region, the drain current linearly increases with $V_G$. Saturation regime is reached when the drain voltage becomes similar to the gate voltage. At this state, the drain current levels out because the channel is *pinched off*, which means charge carriers deplete out at the drain (Figure 11). Mobility ($\mu$) in the saturation region can be found by finding the slope of $|I_D|^{\frac{1}{2}}$ vs $V_G$ plot. High electric fields in the source and drain

regions tend to affect mobility in the linear regime.[30-31] Technically, mobility in linear regime should be similar to mobility in saturation regime. However, due to above restrictions in the linear regime, in this thesis, OFET mobility is calculated in the saturation regime. Moreover, even though the mobility is dependent on gate voltage, Equation 5 and 6 neglects this effect. We assume this dependence is minimal and used the above equations directly.

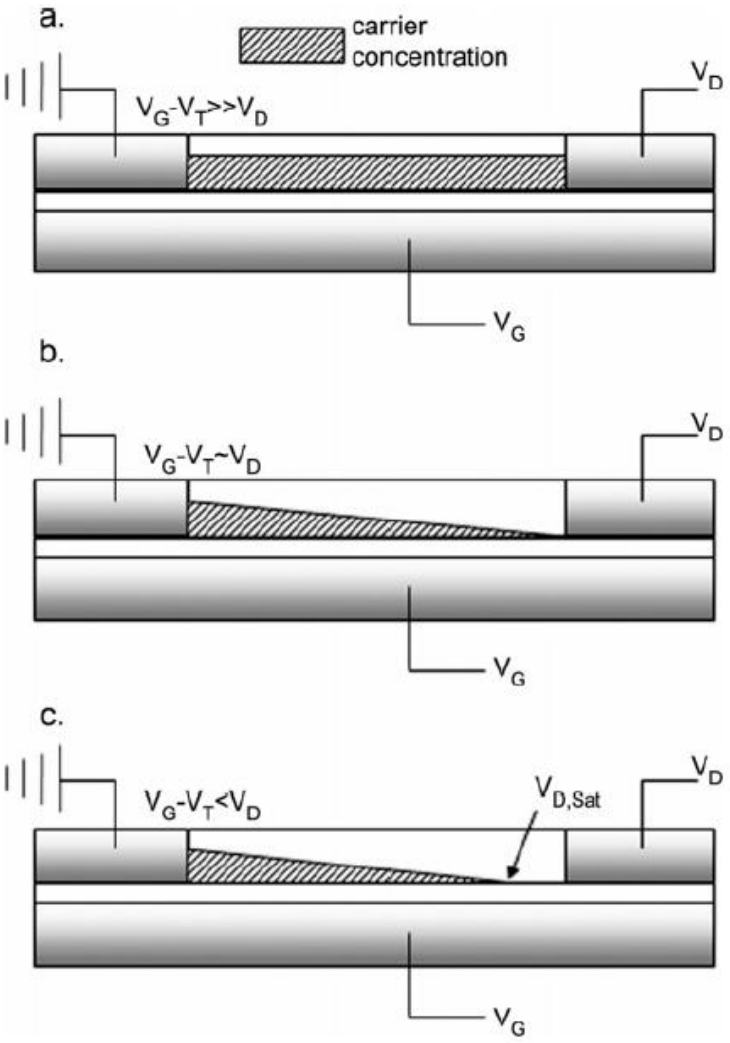


**Figure 11: (a)** Charge carrier concentration profile in linear regime, (b) At pinch point where $V_D \approx V_G - V_T$, carrier concentration depletes out at the drain, (c). Charge carrier concentration profile in saturation regime. Image from[32]

Two major plots are drawn to characterize performance of OFETs: output and transfer curves. The output curve, which plots $I_D$ vs. $V_D$ at a fixed gate voltage $V_G$, shows general characteristics of the current-voltage relationship. (Figure 12 a) In addition, the transfer curve plots $I_D$ vs. $V_G$ at a fixed $V_D$ (e.g. $V_D$ = - 80V) and outlines how efficiently s device can be turned ON and OFF. If we have a high ON/OFF ratio ($\sim 10^5$ and above), which can be withdrawn from the transfer curve, a device effectively turns ON and OFF.

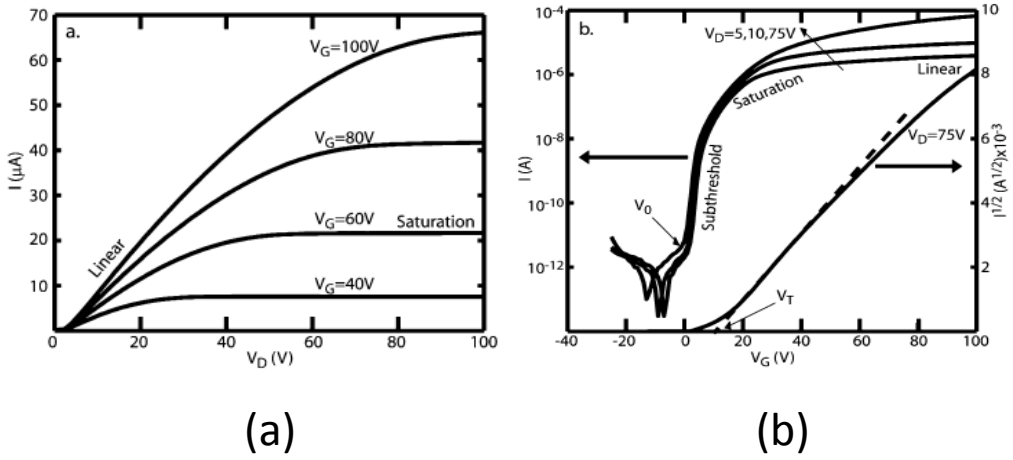


(a) (b)

**Figure 12:** Typical electronic characteristics curves (a) output characteristic curve of OFET and (b) transfer curve of OFET. Image from[32]

## 1.5 Hansen Solubility Parameter

The performance of an OFET is sensitive to slight changes in morphology, aggregation, and other process conditions such as annealing. One of the key ingredients to organic semiconductor processing is the solvent. Depending on the solvent parameters (boiling point, solubility, and polarity etc), OFETs may perform differently. Selecting which solvent to use with certain polymer is challenging. Researchers have consistently put effort in finding relationships and trends associated with solvent characteristics. One of the factors that helps understand the solvent/OSC interaction is solubility parameters ($\delta$).

Solubility parameters, which are frequently known as Hildebrand or total solubility parameters, provide a numerical estimate of how a given solvent and polymer will behave towards each other. A solute is said to be soluble when the solubility parameters of the both solvent and polymer are similar. Also organic solvents have good miscibility and thus, solvents used in this thesis are assumed to be miscible. Total solubility parameters can be represented as Equation 7, where $\Delta H_V$ is the heat of vaporization, *R* is the universal gas constant, *T* is the temperature, *V* is the molar volume, and *E* is the cohesive energy.

$$\delta^2 = \frac{\Delta H_V - RT}{V} = \frac{E}{V} \qquad (7)$$

Cohesive energy density (*E/V*) is the energy required to infinitely separate a unit volume of molecules from their neighboring molecules. The total solubility parameter can be further broken down to specific solubility contributors: dispersion ($\delta_D$), polarity ($\delta_P$), and hydrogen-bonding ($\delta_H$). This contribution is shown in Equation 8.

$$\delta^2 = \frac{E}{V} = \delta_D^2 + \delta_P^2 + \delta_H^2 \qquad (8)$$

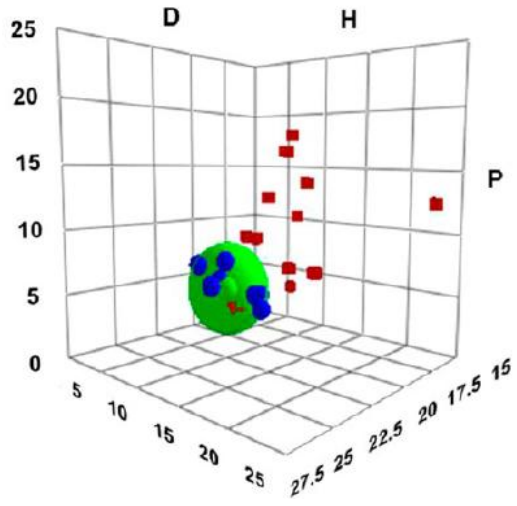


**Figure 13:** The Hansen space drawn in Hansen solubility parameter coordinates where green sphere represents solubility region of P3HT.[33]

Three contributing parameters: the dispersive ($\delta_D$), the polar ($\delta_P$), and hydrogen bonding ($\delta_H$) solubility parameters are set as the Cartesian axis of Hansen space (Figure 13). Solvents that dissolve the polymer generate a sphere with interaction radius, $R_0$. Interaction radius of P3HT is calculated to be 4.20 $MPa^{0.5}$.[33] The center of this sphere determines solubility parameter of the polymer. $R_a$ represents the distance between the solvent and the polymer Hansen solubility parameters as shown in Equation 9, where subscripts 1 and 2 indicate polymer and solvent, respectively.

$$R_a^2 = 4(\delta_{D1} - \delta_{D2})^2 + (\delta_{P1} - \delta_{P2})^2 + (\delta_{H1} - \delta_{H2})^2 \quad (9)$$

$$RED = \frac{R_a}{R_0} \quad (10)$$

Once $R_a$ and $R_0$ are known, the relative energy difference (RED) can be calculated (Equation 10). This measurement provides estimation of miscibility of the solute and polymer. Finally, solvents can be mixed according to Equation 11, as a function of the volume fraction of the components ($\phi_j$) where *x* represents three contributors of Hansen parameters and *j* indicates the solvent species. In this experiment, RED values are fixed by mixing solvents together.

$$\delta_x = \sum (\delta_x)_j \phi_j \quad (11)$$

## 1.6 Motivation and outline of thesis

Organic electronics has been stably studied for more than fifty years; however, there are hindrance for commercialization, yet, despite of its unique characteristics. This is because inorganic materials such as silicon exhibit much stable and higher performance than organic materials. The causes of the inferior performance are primarily relatively low field effect mobility, low stability of polymers in ambient condition, challenges to control the morphology of the film, and many unknown trends of charge transport in different process conditions.

There are many ways to process organic polymers to a thin film on a device. For example, spin-coating method, as its name suggests, uses a radial force from the spinning motion to form evenly distributed films. Drop-casting method simply drops the solution on a device and utilizes evaporation to deposit polymers. The two processing methods result in large difference in the performance of the devices. Likewise, the performance of device varies immensely with change in processing conditions. Therefore, in this thesis, impact of the modification in process parameters such as boiling point, solubility, and polarity will be studied. The P3HT is used as a model to develop trends and correlations from the impacts.

Chapter 2 outlines the impact of how small addition of good solvents to P3HT solution based on chloroform on the device performance. Chapter 3 explores the 'solvent assisted' processing method in more systematic variation in parameters such as boiling points, solubility, and polarity of the second assisted solvents. Overall, the thesis will highlight how the changes in process or solvent parameters will affect the film morphology and charge transports.

# CHAPTER 2

# HIGH BOILING GOOD SOLVENTS EFFECT ON THE MORPHOLOGY AND THE CHARGE TRANSPORT OF P3HT

## 2.1 Introduction

Conventionally, P3HT film OFET is processed with chloroform. This pristine film provides evenly distributed coating and dry quickly due to relatively low boiling point of solvents. The solution processed film is typically semi-crystalline. In the chloroform based pristine film, there is more amorphous region than the crystalline region, so the performance of OFET is low. The pristine film OFET acts as benchmark to compare OFETs processed in different conditions.

There have been many studies to improve the performance of the devices by changing molecular and process parameters. Molecular parameters include molecular weight (MW) and regioregularity (RR).[27,34-36] It is suggested that higher MW material have long polymer chain length, which can connect crystalline domains that are usually separated by relatively low conductive amorphous domains. In addition, increase in RR reduces the reorganization energy, which enhances charge mobility. Process parameters, on the other hand, are film deposition method, solvent boiling points, solubility and other processing conditions. These parameters are also known to affect the assembly of the π-conjugated polymers.

Yang et al. have shown that different solvents have impact on the film structure and hence, influence the morphology and charge transport of the devices.[37] Furthermore, it is also reported that small addition of poor solvent improves molecular structure and mobility in OFET.[38-40] According to Cho et al. using poor solvents that have lower boiling point than the main solvent (e.g. chloroform) have no effect on the film condition

and performance.[41] However, when poor solvents that have higher boiling point than the main solvent were used, polymers aggregated as solvents evaporate during spin-coating method.[41-42] This phenomena is a result of slower evaporation of poor solvents compared to the main solvent. The remaining poor solvents stimulated further aggregation. The uses of high boiling point solvents in the process forms more crystalline film structure because of slow evaporation rate, thus increasing the field effect mobility.[42]

In comparison to the high boiling poor solvents, effect of high boiling good solvents is studied in this chapter. Typical industrial high boiling good solvent is dichlorobenzene, which is well known for its strong solubility and provides crystalline pristine film due to slow evaporation time. However, employing high boiling point solvents in the industry is not practical, because it is toxic and is costly to build process that can anneal in high temperatures. Also dichlorobenzene is poor polar index solvent that has poor wetting on silicon oxide wafer. Therefore, deposited films are inhomogeneous and very thin, unless self-assembled monolayer (SAM) is pre-deposited to the wafer.[43]

In this chapter, we suggest a unique method to control dichlorobenzene by mixing with chloroform. By doing so, we improved wetting of P3HT film and constructed nano-fibers that enhanced the mobility of the OFET by five times the mobility of pristine film devices. The spectroscopic evidence supports that processed film contains nano-fiber structure that is not present in the pristine film. Also lower annealing temperature is required to dry film; hence, the process is more cost effective. This study provides a method to control a poor wetting solvent in processing high performing films. Also ortho-dichlorobenzene (*o-DCB*) and meta-dichlorobenzene (*m-DCB*) are compared to view solubility and polarity effects.

## 2.2 Experimental Procedures

### *2.2.1 Materials*

The P3HT (catalog no. 445703), chloroform (anhydrous grade), ortho-dichlorobenzene, meta-dichlorobenzene were purchased from Sigma Aldrich and used without further purification. The P3HT had a measured Mw of 50.7kDa with respect to polystyrene standards as determined by Gel Permeation Chromatography (waters 1515 Isocratic HPLC equipped with a Waters 2489 UV/vis detector and Styragel HR 5E column) using tetrahydrofuran(THF) as the effluent. Also the head to tail regioregularirty of approxmiately 97%.

### *2.2.2 Organic Field-Effect Transistor (OFET) Fabrication and Characterization*

A bottom-contact FET was fabricated to characterize electrical properties of the P3HT films, which were spin-coated on 300nm thick $SiO_2$ gate dielectric. The device contains three contact regions: the source and the drain electrodes from deposition of Au/Cr on the gate dielectric, and gate electrode made of highly doped silicon wafer. The source and drain electrodes are deposited using a standard photolithography based lift-off process followed by evaporation of 50 nm Au contacts with 3nm of Cr as the adhesion layer using E-beam (Denton Explorer). Before spin-coating P3HT solutions, devices are cleaned with acetone in an ultrasound cleaning bath followed by rinsing with methanol and isopropanol. After that all devices are treated for 15 min in a UV-ozone cleaner (Novascan PSD-UV) to completely remove the residual photoresists and other contaminant. After the cleaning process, substrates were hydrophilic. P3HT solutions are prepared in ambient conditions, by dissolving 10mg of P3HT in 2ml of $CHCl_3$ base solvents containing small amount of o-DCB or m-DCB (0, 1, 2, 3, 5 vol %) at ca. 50℃. Then transistors are prepared by spin-coating (WS-650MZ-23NPP, Laurell) the solution on the cleaned substrates at a spin speed of 1500 RPM for 60s in air. The electrical properties are characterized in nitrogen ambient using an Agilent 4155C semiconductor

parameter analyzer. The carrier mobility was obtained in saturation region, where drain voltage was set as -80V. Mobility was calculated by plotting the $I_D$ vs. $V_G$ and fitting the data to the Equation 6 shown in previous chapter, where capacitance per unit area of $SiO_2$ gate dielectric is $1.15\times10^{-8}\,Fcm^{-2}$, W is 2000 $\mu m$, and L is 50 $\mu m$.

$$I_{D,Sat}=\left(\frac{1}{2}\right)\frac{W}{L}\mu C_{OX}(V_G-V_T)^2 \quad \text{for } V_D \geq V_{Dsat}=V_G-V_T \tag{6}$$

*2.2.3 UV-Vis Spectra of P3HT*

Both the solution and solid state of P3HT were used to find UV-Vis spectra by using an Agilent 8510 Spectrophotometer. Solutions are dropped to a UV-vis vial and solid state films are spin-coated on treated glass-slides.

*2.2.4 Grazing Incidence X-Ray Diffraction (GIXRD)*

In order to obtain GIXRD data, cleaned hydrophilic silicon oxide substrates were spin-coated with the P3HT solutions. The methods to prepare spin-coated samples are identical to OFET devices. Using Panalytical X'Pert Pro system equipped with a Cu X-ray source operating at 45kV and 40mA, out-of-plane GIXRD data could be obtained. The grazing incidence angle was fixed at 0.2° and the detector was scanned from 3° to 30°. The peak positions were found by fitting the peaks using the analysis software (MDI JADE).

*2.2.5 Atomic Force Microscopy (AFM) studies of P3HT*

The AFM measurements were done on films spin-coated on OFET substrates, with a Bruker Dimension ICON with ScanAsyst® scanning probe microscope in tapping mode with an AFM probe of Tap150 cantilever.

## 2.3 Results and Discussions

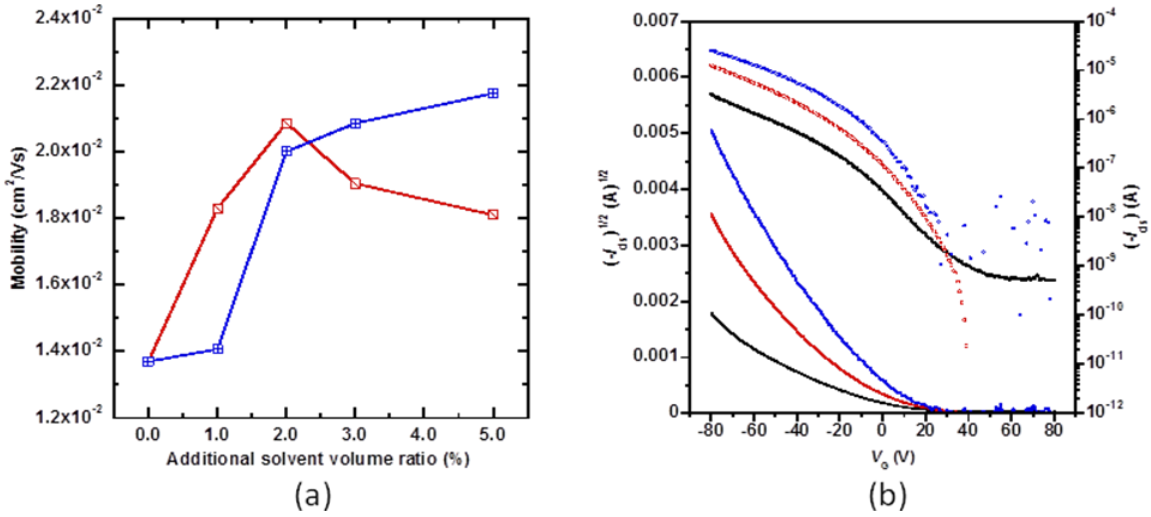


**Figure 14:** (a) Effect of addition of o-DCB (red) and m-DCB (blue) in P3HT solutions on mobility of films. All experiments are performed in ambient condition. (b) Transfer characteristic obtained from 5 vol % of o-DCB and m-DCB P3HT films compared to pristine film.

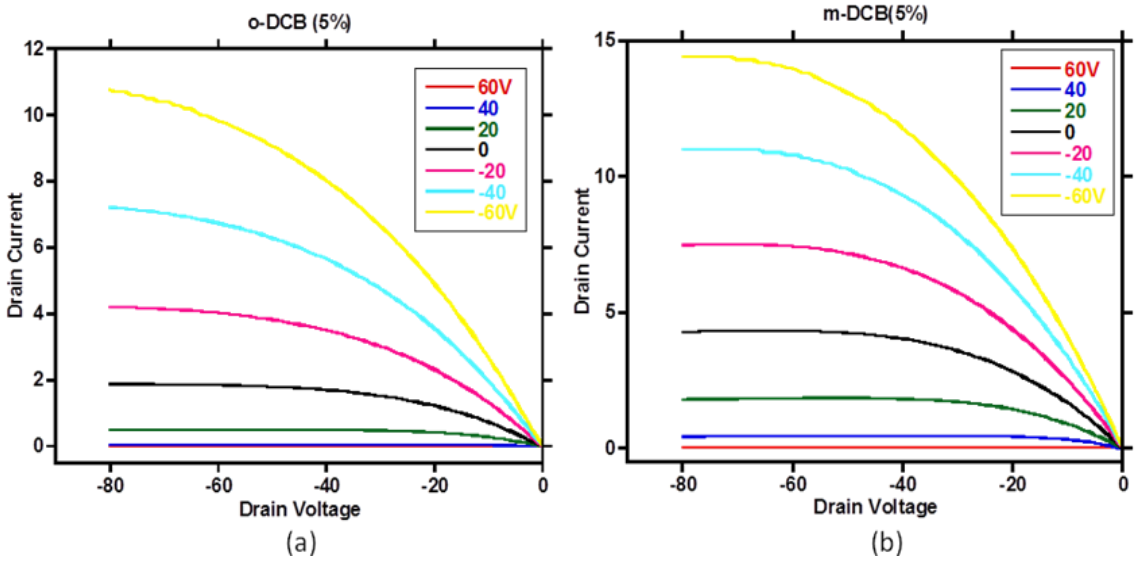


**Figure 15:** Representative output curve of P3HT film processed with (a) o-DCB and (b) m-DCB. The drain current represents minus current in microampere ranges.

Figure 14 shows the average field effect mobilities obtained from P3HT film processed in solvents with 0, 1, 2, 3, and 5 vol % of o-DCB or m-DCB. All P3HT films were deposited by using spin-coating method. The mobility of P3HT varied from

$1.37\pm0.15\times10^{-2}\,cm^2V^{-1}s^{-1}$ for pristine film to $2.09\pm0.09\times10^{-2}\,cm^2V^{-1}s^{-1}$ for 2 vol % of o-DCB P3HT solution. In contrast, the mobility of 5 vol % m-DCB P3HT rose up to $2.18\pm0.23\times10^{-2}\,cm^2V^{-1}s^{-1}$. The increase and difference in mobilities are observable when high boiling good solvents is included as cosolvent. Figure 14 (b), and 15 are representative characteristic curves of P3HT film processed with o-DCB and m-DCB, respectively, that follows the trend of the typical p-type OFET operation in accumulation mode. In addition of both high boiling points, mobility increased by two times the pristine value. The ON/OFF ratio of the devices is visible with the difference of on-current and off-current in Figure 14 (b). The addition of high boiling good solvent as cosolvent provided similar trends of mobility with addition of less volatile poor solvent. The pristine film processed with pure chloroform leads to relatively poor molecular ordering of the polymer chains because of chloroform's fast evaporation during the spin-coating method. Therefore, pristine film provided relatively low mobility[34,41,44]. The film is at semi-crystalline state where both high conductive crystalline and low conductive amorphous state co-exist. Increasing the concentration of o-DCB from 2 to 5 % influenced a decrease in charge mobility, which is a result of more crystalline ordering that formulated grain boundaries in the film.[41] Charges are hindered from transporting due to these rigid interfaces.

On the other hand, although m-DCB have similar boiling point with o-DCB, m-DCB exhibit different polarity and solubility due to differences in molecular structure (Figure 16). Mobility of P3HT coated with cosolvent m-DCB increased gradually, due to the increase in molecular ordering and crystalline structure induced from relatively poor solubility. The solubility test has been conducted as shown in Figure 17. Even though exact solubility of m-DCB is not known, P3HT starts to aggregate and turn solution dark after 2 hours, which shows it has relatively poor solubility than o-DCB.

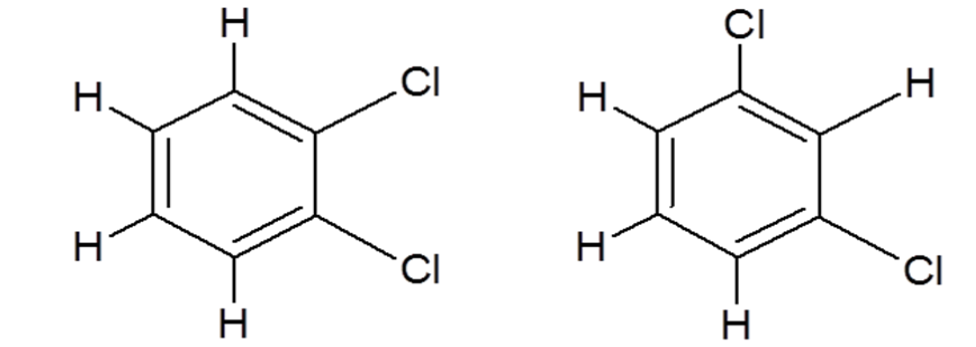


(a) ortho-dichlorobenzene (o-DCB)

(b) meta-dichlorobenzene (m-DCB)

**Figure 16:** Molecular structures of (a) ortho-dichlorobenzene (b) meta-dichlorobenzene.

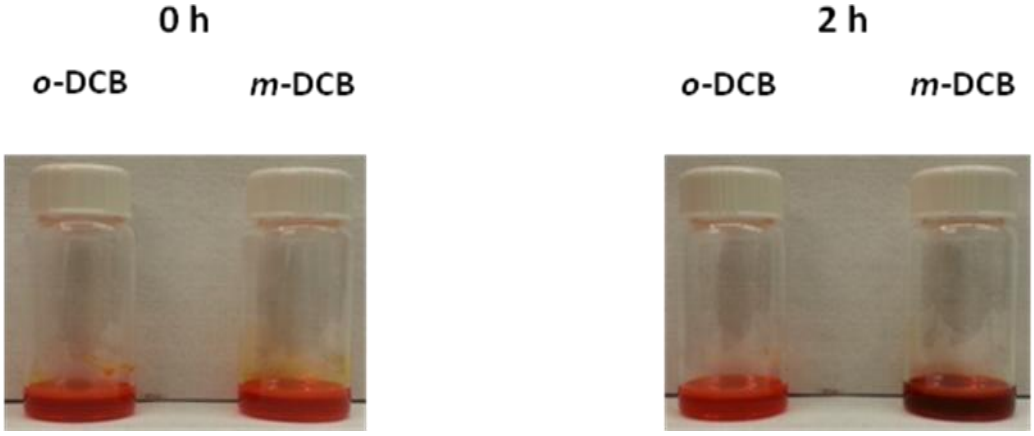


**Figure 17:** Solubility test between ortho- and meta-dichlorobenzene. After two hours, m-DCB solution turned dark orange when o-DCB remained orange.

Figure 18 and 19 depicts the UV-vis absorption spectra of P3HT/chloroform-o-DCB solution and P3HT/chloroform-m-DCB solution with their corresponding solid-state P3HT films, respectively. The absorption maximum, $\lambda_{max}$ ,related to $\pi$-$\pi^*$ intraband transition is shown at ca. 450nm for all P3HT solution state. The subtle differences are observable in the spin-coated P3HT thin-films. In Figure 18 (b) and 19 (b), addition of the cosolvents causes red shift of band at ca. 533nm. Additionally, weak absorption bands are developed at ca. 555 nm and 605 nm, which are due to vibronic side band from

increase in co-facial π-π stacking of P3HT.[45] Therefore, addition of high boiling good solvents to the P3HT solution in chloroform promote orderly π stacking of P3HT chains.

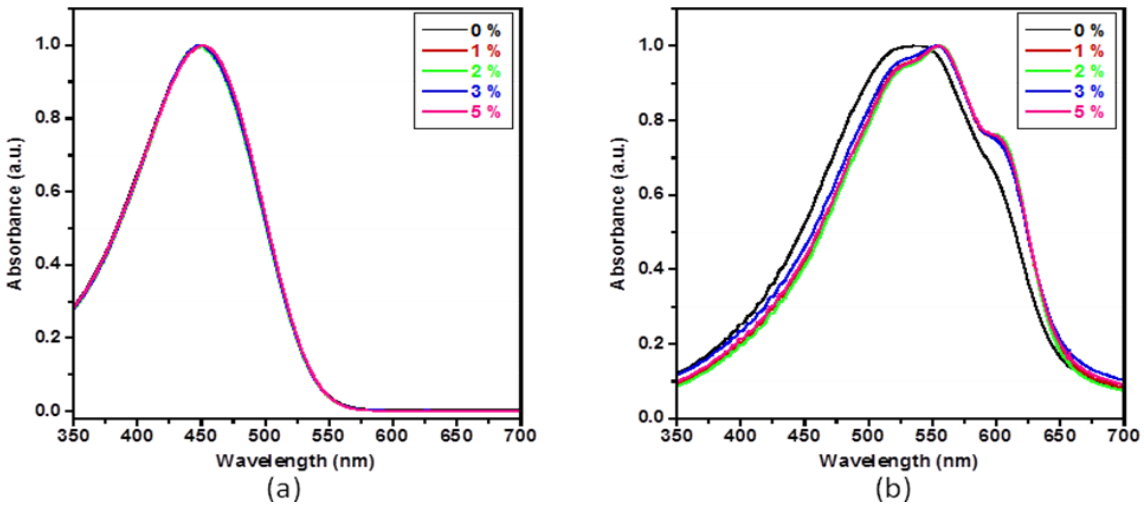


**Figure 18**: Normalized UV-vis absorption spectra of (a) P3HT/solvent solution as a function of volume fraction o-DCB added and (b) corresponding P3HT films fabricated using spin-coating method. For clarity, only the section from 350-700nm is shown.

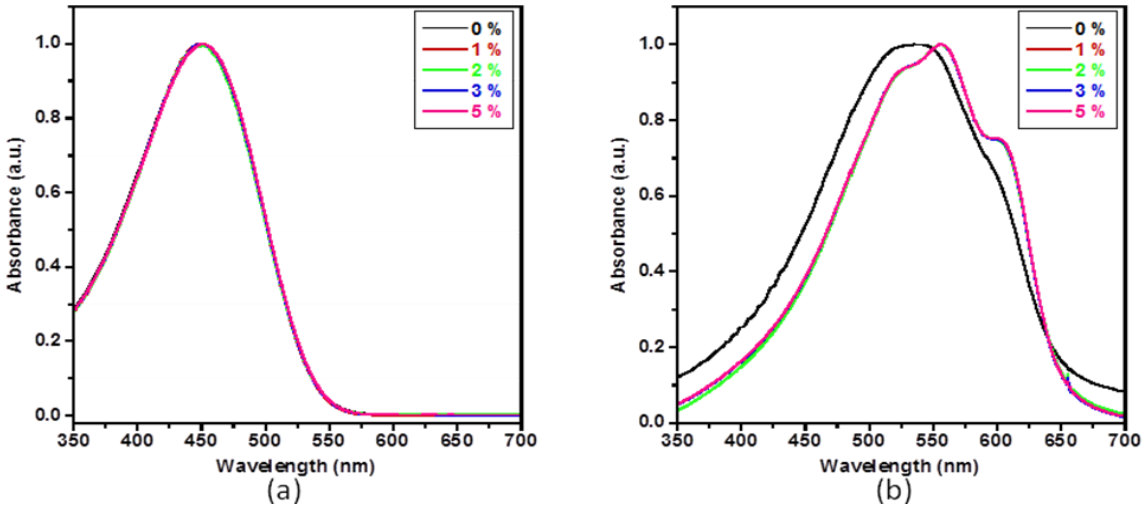


**Figure 19:** Normalized UV-vis absorption spectra of (a) P3HT/solvent solution as a function of volume fraction m-DCB added and (b) corresponding P3HT films fabricated using spin-coating method. For clarity, only the section from 350-700nm is shown

Direct comparison between the morphology of P3HT film processed with o-DCB and m-DCB is made in Figure 20. Both DCB processed P3HT films showed a red-shift of absorption maximum from the pristine P3HT film. Absorption wavelengths below and

above maximum absorption wavelength, $\lambda_{max}$, represent amorphous and crystalline regions, respectively. The development of crystalline region on film indicates the presence of orderly packing of P3HT chains.[46] Films processed in m-DCB have peaks red shifted and have lower intensity of amorphous region than film processed in o-DCB. Thus, m-DCB processed P3HT films have more crystalline regions, which are expected to be an indication of enhanced intermolecular interactions between P3HT chains.[47]

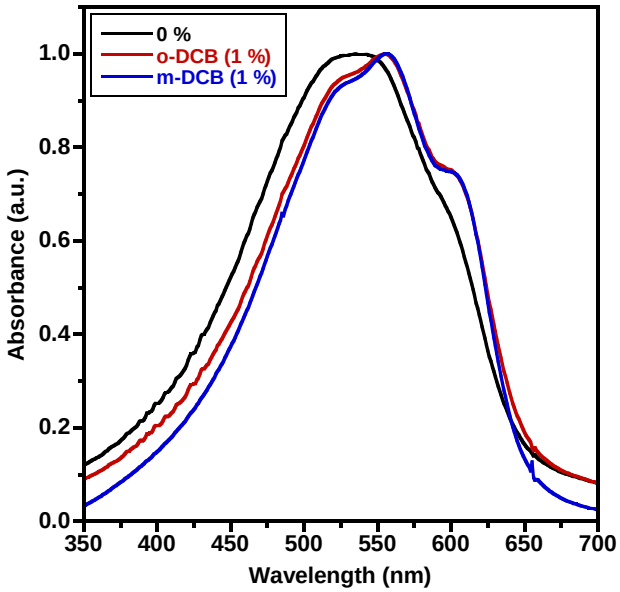


**Figure 20:** UV-vis spectra comparison between the molecular interaction between P3HT processed in o-DCB mixture and m-DCB mixture

In addition to intermolecular interaction between the polymer chains, we can also observe the conjugation length or intra-molecular interaction changes between the films processed with different co-solvents using Spano's Model.[46] Spano model explains the development of crystalline region by weakly interacting H-aggregate (blue shifting) states. The vibronic bands are caused by interchain coupling and further associated to free excitonic bandwidth (W) that indicates the conjugation length of a polymer chain.[34, 46, 48] W are correlated to ratio between the intensities of the (0-1) and (0-1) transition bands as shown in Equation 12, where $A_{0-0}$ and $A_{0-1}$ are the intensities of the (0–0) and (0–1)

transitions, respectively and $E_P$ is the vibrational energy of the symmetric vinyl stretch, which is assumed to be 0.18 eV.[46]

$$\frac{A_{0-0}}{A_{0-1}} \approx \left( \frac{1 - 0.24W / E_p}{1 + 0.073W / E_p} \right)^2 \qquad (12)$$

When value of W falls, average conjugation length and chain order increases [34,46], thus, indicating enhanced intra-molecular chain ordering. According to Figure 21, where experimental UV-vis data are fitted to the Spano model, there is 20 meV difference in W value between the pristine film and cosolvent processed films. Therefore, intrachain ordering has been enhanced with addition of cosolvent in processing P3HT film. Also m-DCB P3HT film has lower W value than o-DCB P3HT film, which is an indication of highly ordered packing and stronger intra-molecular interaction in m-DCB processed films.

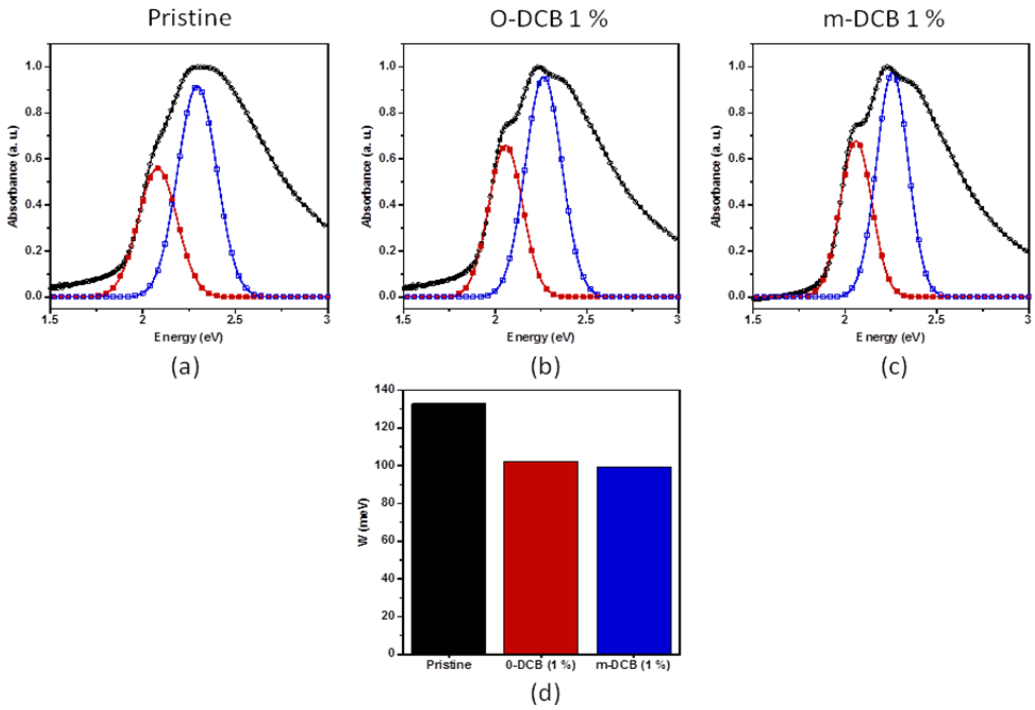


**Figure 21:** UV-vis spectrum of (a) pristine, (b) 1% o-DCB cosolvent, and (c) 1% m-DCB cosolvent processd P3HT films analyzed with Spano model. (d) shows the band energy (W) of the three films.

The enhanced crystallinity of P3HT is also supported by X-ray diffractograms obtained from grazing incidence (GIXRD). Figure 21 shows the increase in intensity of the (100) peak as co-solvent concentration increases. (100) peak is related to lamellar packing of the polymer chains directing orthogonal to the main backbone of P3HT.[49] This increase may be due to increase in size and number of crystallites presented in the P3HT film.[50] Both P3HT films processed with hundred percent of o-DCB and m-DCB showed small development of the (100) peak. This can be explained with relatively thin film thickness due to poor wetting property resulted from weak polarity of the solvents. The wetting of non-polar P3HT solute is poor when non-polar (hydrophobic) solvent is used to process the film on the hydrophilic surface of substrate.

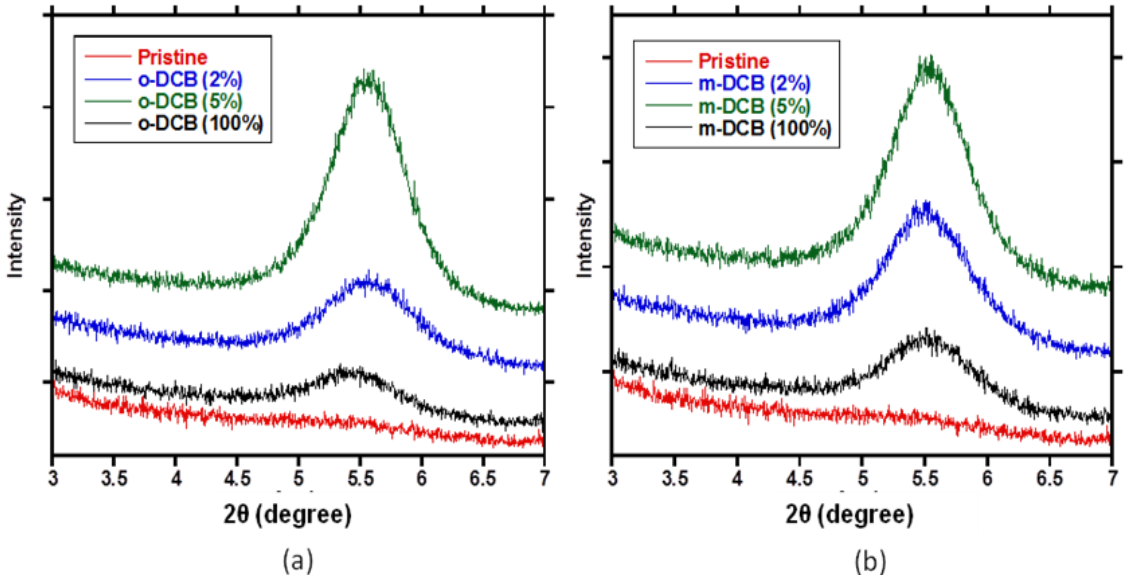


**Figure 22:** Grazing incidence X-Ray diffraction profiles of P3HT films processed with (a) o-DCB and (b) m-DCB mixed solutions.

The influence of the molecular change of P3HT structure on macroscopic morphology of the film can be observed with atomic force microscopy (AFM). Compared to initial featureless pristine film, the addition of co-solvents induced fibrous structure formation, as well as, increasing the crystallinity and roughness of the film. The

fibrous lateral order is expected to cause more efficient charge transport[37, 51]. The morphology of the P3HT film prepared with 100% dichlorobenzene showed an aggregation of P3HT fiber cause by slow evaporation of high boiling solvent during the spin-coating deposition. The nano-fibrous textures are expected to have appeared due to this difference in evaporation rate of chloroform (fast) and dicholorobenzene (slow) affecting aggregation of P3HT solutes. During the spin-coating process, P3HT concentration may have been much higher in good solvent dichlorobenzene than relatively good solvent chloroform. These separations of P3HT concentration and difference in evaporation rate have caused the change in morphology of the thin film, hence, affecting the field-effect mobility of the devices. P3HT film prepared with m-DCB enhanced crystallinity more than o-DCB. The difference is explained with relatively poor solubility of m-DCB than o-DCB. This enhanced crystallinity and formation of fibrous morphology due to addition of m-DCB, caused higher OFET performance than device coated with P3HT film processed in o-DCB.

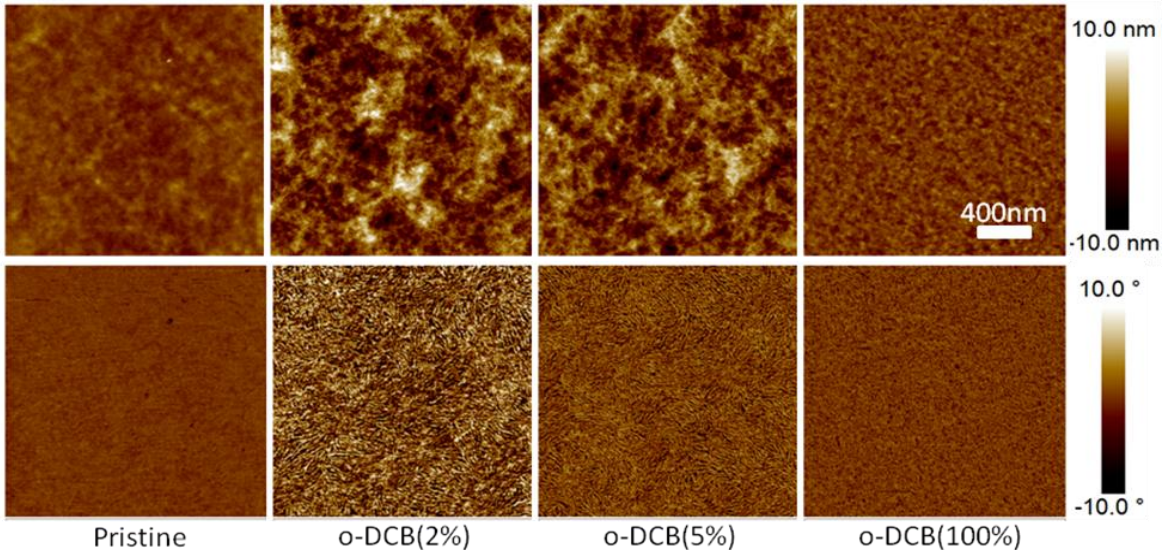


**Figure 23:** Tapping mode AFM images of 0, 2, 5, and 100 % addition of o-DCB. Upper row shows the height image and the lower row represents phase image of the P3HT films. The scan area of phase and height images are $2\ \mu m \times 2\ \mu m$.

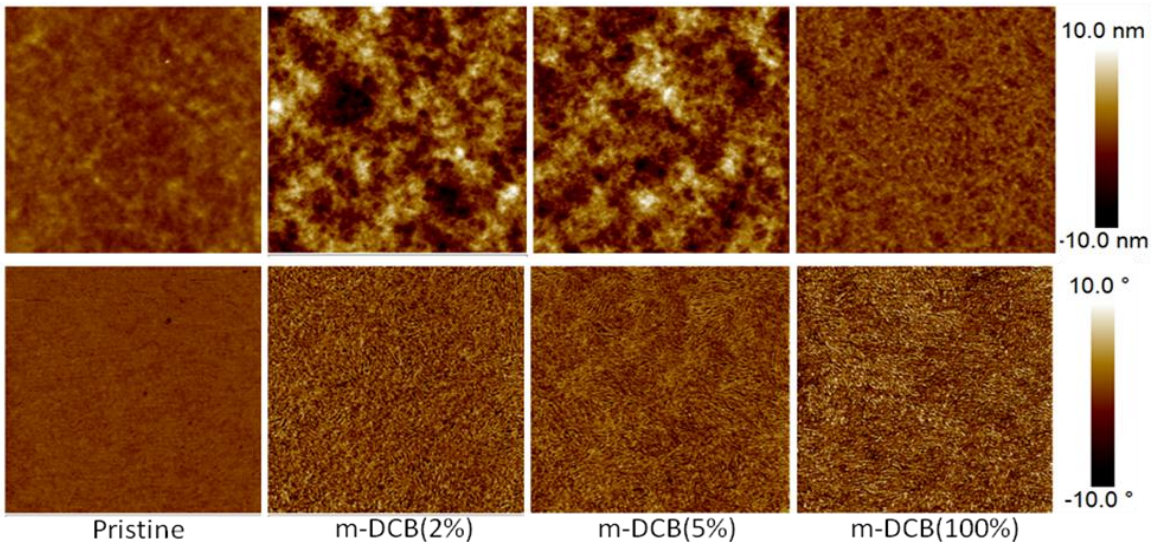


**Figure 24:** Tapping mode AFM images of 0, 2, 5, and 100 % addition of m-DCB. Upper row shows the height image and the lower row represents phase image of the P3HT films. The scan area of phase and height images are $2\,\mu m \times 2\,\mu m$.

Not only the mixture of o-DCB and m-DCB increase the morphology and electronic properties of P3HT film, the process enhanced wetting of the P3HT film. Although non-polar DCB effectively dissolves non-polar P3HT, the solvent has poor interaction with hydrophilic surface of substrate. We can visualize that wetting of P3HT film prepared with pure o-DCB and m-DCB solution are poor on the substrates as shown in Figure 25. When DCB is mixed with chloroform, relatively higher polar index solvent, wetting is improved as visualized in Figure 25. This improvement is expected to be caused by relatively polar chloroform solvent interacting with polar surface of the substrate.

Previously, we have reported OFET performance with o-DCB processed P3HT film decreased after addition of 2% o-DCB because of increase in aggregation and grain boundaries that trapped charges from transporting. P3HT dissolved in m-DCB has better wetting property than P3HT dissolved in o-DCB. As a result of better wetting, m-DCB processed P3HT has more homogeneous film. The superior mobility shown by m-DCB

processed film is due to this homogeneity of the film and enhanced crystalline ordering induced by relatively poor solubility.

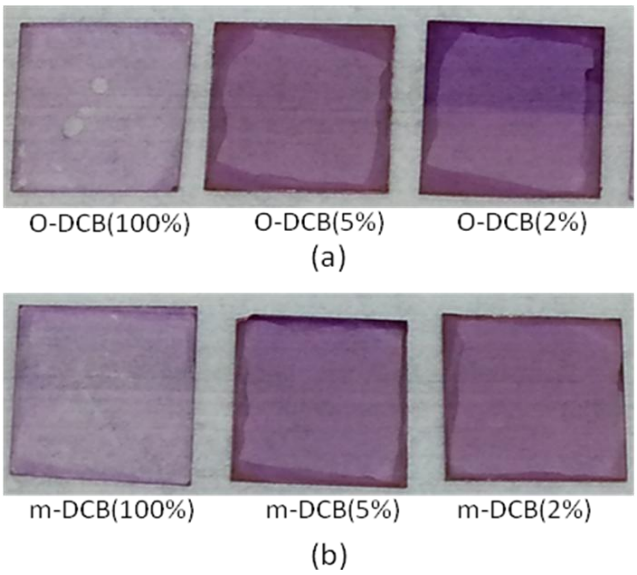


**Figure 25:** Wetting image of (a) o-DCB and (b) m-DCB processed P3HT film on a pre-clean glass plate.

## 2.4 Conclusion

In this chapter, we have investigated how addition of high boiling good solvents will have impact on the morphology and electronic properties of P3HT film OFET. Previously, SAM layers had to be deposited on a substrate to enhance wetting of P3HT processed with DCB. Also DCB required high annealing condition to dry the film. By mixing DCB to chloroform, wetting property improved and less annealing temperature was required to make OFET. Addition of o-DCB and m-DCB improved the ordered aggreagtion of the thin film. P3HT film processed with m-DCB performed better mobility than P3HT film made with o-DCB cosolvent. This improvement by m-DCB was because of relatively homogeneous thin film promoted by polarity difference. Even though chlorine based solvents are still inhibited to be used in industrial applications, this research can be used as an example to improve the device performance by mixing solvents to process organic semiconductor films.

# CHAPTER 3

# SYSTEMATIC STUDY OF SOLVENT ASSISTED RE-ANNEALING TREATMENT AFFECTING THE P3HT FILM MORPHOLOGY AND THE ELECTRONIC PROPERTIES

Solution processable OFETs have drawn significant attention for their unique solution rheology and physical properties.[52] However, the mobility of polymer based OFETs is still not comparable to molecular semiconductor based OFET.[53] Also fast degradation time of polymer in ambient condition is another big barrier for polymer OFET to be used in further industrial application.

Improvements in molecular ordering of polymers are known to increase the performance of the OFET. One of the main factors to impact molecular ordering is solvent parameters. Solvent parameters such as boiling point and polarity are known to influence the molecular self-ordering time and wettability of polymer solutions on substrates.[22,54] With these modifications of parameters film molecular packing can be changed, as a result, affecting the characteristics of the devices.

Along with controlling solvent parameters, solvent assisted re-annealing treatment was discovered to be an effective technique to improve overall performance of OFET. This treatment drops a secondary solvent as soon as polymer film is coated on substrates. According to Di et al. solvent-assisted re-annealing treatment provided multi-functional applications such as encapsulating organic polymer and depositing top-contact gates.[55] In their research, solvents with different polarity, boiling point, and solubility were selected as assisting solvents, which included high boiling point solvents like dichlorobenzene that requires high annealing temperature of 170℃. Therefore, the process cannot be commercialized for industrial applications.

In this thesis, systematic study of solvent-assisted re-annealing treatment is conducted by controlling the boiling point, polarity and solubility of solvents. The result showed that non-polar assisted solvents provided much higher impact in mobility than polar assisted solvents. Also lower boiling point temperature solvents had relatively, smaller influence on the device morphology and charge transport than higher boiling temperature solvents.

## 3.2 Experimental Procedures

### *3.2.1 Materials*

The P3HT (catalog no. 445703), chloroform (anhydrous grade), tetrahydrofuron (THF), methanol, hexane, toluene, 2,5-dimethylhexane were purchased from Sigma Aldrich and used without further purification. The P3HT had a measured Mw of 50.7kDa with respect to polystyrene standards as determined by Gel Permeation Chromatography (waters 1515 Isocratic HPLC equipped with a Waters 2489 UV/vis detector and Styragel HR 5E column) using tetrahydrofuran(THF) as the effluent. Also the head to tail regioregularity approximately 97%.

### *3.2.2 Organic Field-Effect Transistor (OFET) Fabrication and Characterization*

A bottom-contact FET was fabricated to characterize electrical properties of the P3HT films, which were spin-coated on 300nm thick $SiO_2$ gate dielectric. The device contains three contact regions: the source and the drain electrodes from deposition of Au/Cr on the gate dielectric, and gate electrode made of highly doped silicon wafer. The source and drain electrodes are deposited using a standard photolithography based lift-off process followed by evaporation of 50 nm Au contacts with 3nm of Cr as the adhesion layer using E-beam (Denton Explorer). Before spin-coating P3HT solutions, devices are cleaned with acetone in an ultrasound cleaning bath followed by rinsing with methanol and isopropanol. After that all devices are treated for 15 min in a UV-ozone cleaner

(Novascan PSD-UV) to completely remove the residual photoresists and other contaminant. After the cleaning process, substrates were hydrophilic. P3HT solutions are prepared in ambient conditions, by dissolving 10mg of P3HT in 2ml of $CHCl_3$ base solvents ca. 50℃. Then transistors are prepared by spin-coating (WS-650MZ-23NPP, Laurell) the solution on the cleaned substrates at a spin speed of 1500 RPM for 60s in air. Then secondary solvents that are classified according to their boiling point (60℃ and 110℃) and polarity are mixed to match RED values of 1.8, 2.0, and 2.2. The secondary solvents, including pure good and poor solvents are dropped on the coated P3HT film. The electrical properties are characterized in nitrogen ambient using an Agilent 4155C semiconductor parameter analyzer. The carrier mobility was obtained in saturation region, where drain voltage was set as -80V. Mobility was calculated by plotting the $I_D$ vs. $V_G$ and fitting the data to the Equation 6 shown in previous chapter, where capacitance per unit area of $SiO_2$ gate dielectric is $1.15\times10^{-8}\,Fcm^{-2}$.

$$I_{D,Sat}=\left(\frac{1}{2}\right)\frac{W}{L}\mu C_{OX}(V_G-V_T)^2 \quad \text{for } V_D \geq V_{Dsat}=V_G-V_T \tag{6}$$

*3.2.3 UV-Vis Spectra of P3HT*

Solid state of P3HT was used to find UV-Vis spectra by using an Agilent 8510 Spectrophotometer. Solutions are spin-coated on treated glass-plates.

*3.2.4 Thickness of P3HT film*

J.A. Woollam V-VASE variable angle spectroscopic ellipsometer were used to measure the thickness of the coated P3HT film. The film are spin-cated on a reflective silicon dioxide substrate.

*3.2.5 Atomic Force Microscopy (AFM) studies of P3HT*

The AFM measurements were done on films spin-coated on OFET substrates, with a Bruker Dimension ICON with ScanAsyst® scanning probe microscope in tapping mode with an AFM probe of Tap150 cantilever.

## 3.3 Results and Discussion

Secondary assisted solvents are prepared by using Hansen solubility parameters. The solvents are divided into their boiling points and polarity. Good solvents are mixed with the poor solvents to provide fixed relative energy difference (RED) values. Solubility, which is represented with RED values are set to values that would not completely wash the P3HT film off the substrate. The volume ratios of mixed solvents are provided in Table 1.

**Table 1:** Conversion of volume ratio to fixed RED values of 1.8, 2.0 and 2.2.

| **Solvent Mixtures (Good/Poor)** | **Solvent volume ratio (v/v)** | ***D*** **(MPa$^{1/2}$)** | ***P*** **(MPa$^{1/2}$)** | ***H*** **(MPa$^{1/2}$)** | **RED** |
|---|---|---|---|---|---|
| THF/Methanol | 94/6 | 16.7 | 6.1 | 8.9 | 1.80 |
| | 88/12 | 16.5 | 6.5 | 9.7 | 2.00 |
| | 82.2/17.8 | 16.4 | 6.9 | 10.5 | 2.20 |
| THF/Hexane | 45/55 | 15.8 | 2.6 | 3.6 | 1.80 |
| | 31/69 | 15.5 | 1.8 | 2.5 | 2.00 |
| | 19/81 | 15.3 | 1.1 | 1.5 | 2.20 |
| Toluene/DMH | 37.5/62.5 | 16.0 | 1.5 | 2.4 | 1.80 |
| | 23/77 | 15.5 | 1.5 | 2.5 | 2.00 |
| | 18.5/91.5 | 15.1 | 1.5 | 2.5 | 2.20 |

**Table 2:** Solubility parameter test of P3HT in multiple organic solvents.

| **Solvents** | **P3HT (mg/mL)** |
|---|---|
| Chloroform | > 5 |
| Hexane | < 1 |
| Dimethyl Sulfoxide (DMSO) | < 1 |
| Dimethyl Formamide (DMF) | < 1 |
| N-Methyl-2-Pyrrolidone (NMP) | < 1 |
| Acetonitrile | < 1 |
| Acetone | < 1 |
| Cyclohexanone | < 1 |
| Benzyl Alcohol | < 1 |
| Tetrahydrofuran (THF) | 1 – 3 |
| *o-Dichlorobenzene* | > 5 |
| *p-Xylene* | 1 – 3 |
| Methanol | < 1 |
| Trichloroethylene | > 5 |
| 1,2,4-Trichlorobenzene | > 5 |
| Chlorobenzene | > 5 |
| Toluene | 2 – 4 |
| Carbon Disulfide | > 5 |
| Diethyl Ether | < 1 |
| Thiophene | > 5 |
| Pyridine | < 1 |
| 2,5-dimethylhexane | < 1 |

Table 2 displays the solvents used to find the radius of Hansen sphere ($R_o$), which was calculated to be 4.20 $MPa^{1/2}$. This $R_o$ was used to calculate RED values.

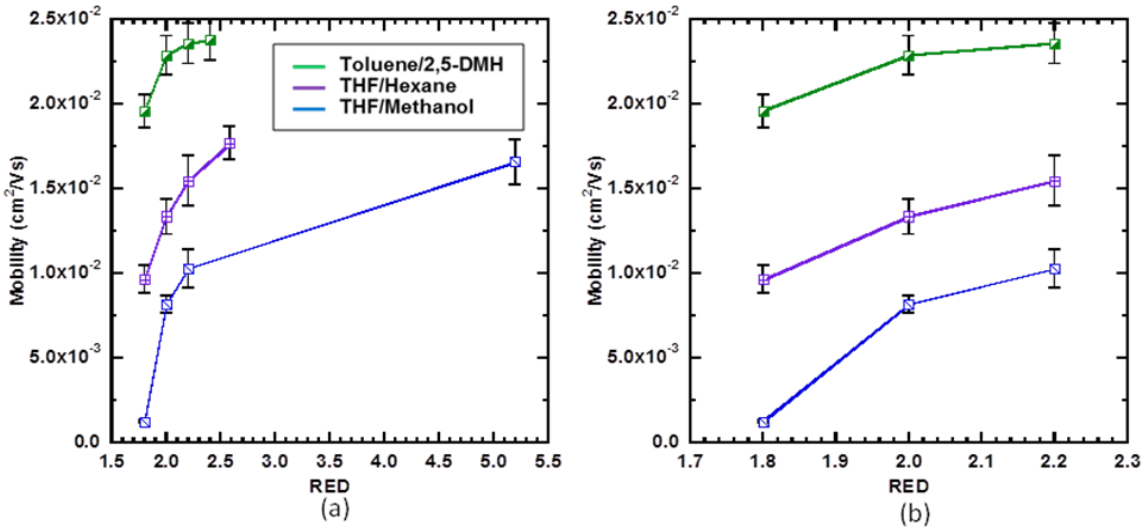


**Figure 26:** (a) Mobility of OFET processed with secondary solvents. (b) Mobility of controlled range of RED value (1.8, 2.0 and 2.2).

Figure 26 shows the electronic characteristics of device prepared with varying secondary solvents. As represented on Figure 26 (a) and (b), there is an increase in trend of mobility as RED values increase. This means mobility of OFET rose as solubility of secondary solvent decreased. Devices prepared with Toluene/2,5-dimethylhexane provided highest mobility of $2.36 \pm 0.16 \times 10^{-2} cm^2 V^{-1} s^{-1}$ where the pristine film mobility, in average, was $1.44 \pm 0.11 \times 10^{-2} cm^2 V^{-1} s^{-1}$. The P3HT dissolved in chloroform, results in film rich with low conductive amorphous region.[27,35]. Mainly understood by poor structured molecular ordering of the polymer chains that consequence in low mobility.[34,41, 44] The low charge transport in low RED, is expected to be influence of interfaces between the grains. The soluble secondary solvents impacts the film and causes inhomogenity in the results P3HT film.[41] Thus, the solubility effect of secondary solvents may increase crystallinity of the P3HT film, it leads to formation of interfaces between the crystalline regions, which hinders efficient charge transport. The trend of charge transport mobility will be further investigated with morphology of the film.

Furthermore, Figure 27 (a) and (b) shows the representative transfer curve and output characteristics curves of P3HT OFETs fabricated with solvent-assisted technique.

The solvent-assisted processed OFETs provided relatively low ON/OFF ratio compared to the pristine, which may be due to influence of secondary solvents forming inhomogenity on the P3HT thin film.

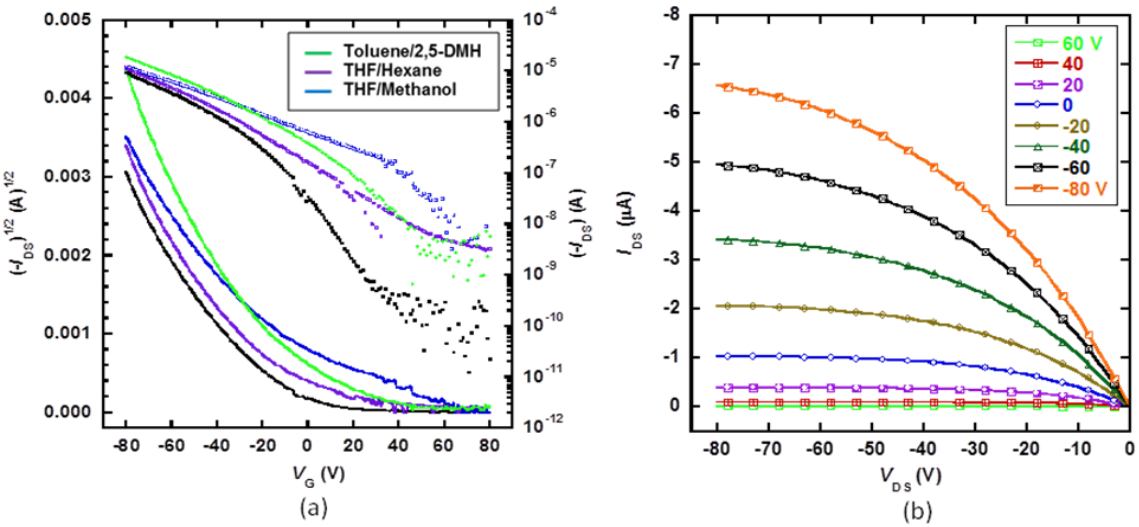


**Figure 27:** (a) Transfer characteristics of P3HT film OFETs treated with specified secondary solvents. (b) Representative output characteristic curve obtained from P3HT OFET fabricated by spin-coating of P3HT dissolved in chloroform. All the OFETs were fabricated in the air and all measurements were taken inside a nitrogen glovebox.

The molecular change of P3HT film can be observed using UV-vis spectrum as shown in Figure 28. The absorption maximum, $\lambda_{max}$ ,related to $\pi$-$\pi^*$ intraband transition is shown at ca. 533 nm. The spectrums showed a red shift of the 533nm peak as to decrease in RED value (increase in solubility) of the assisted solvents. Additionally, weak absorption bands have developed at ca. 555 nm and 605 nm, which is due to vibronic side band from increase in co-facial $\pi$-$\pi$ stacking of P3HT.[45] The secondary solvent that has relatively high solubility dissolved the surface of the film, which impacted the crystallinity. However, the OFET provided very low mobility when low RED was used, from which we can expect inhomogenity in P3HT film due to irregular influence of secondary solvents.

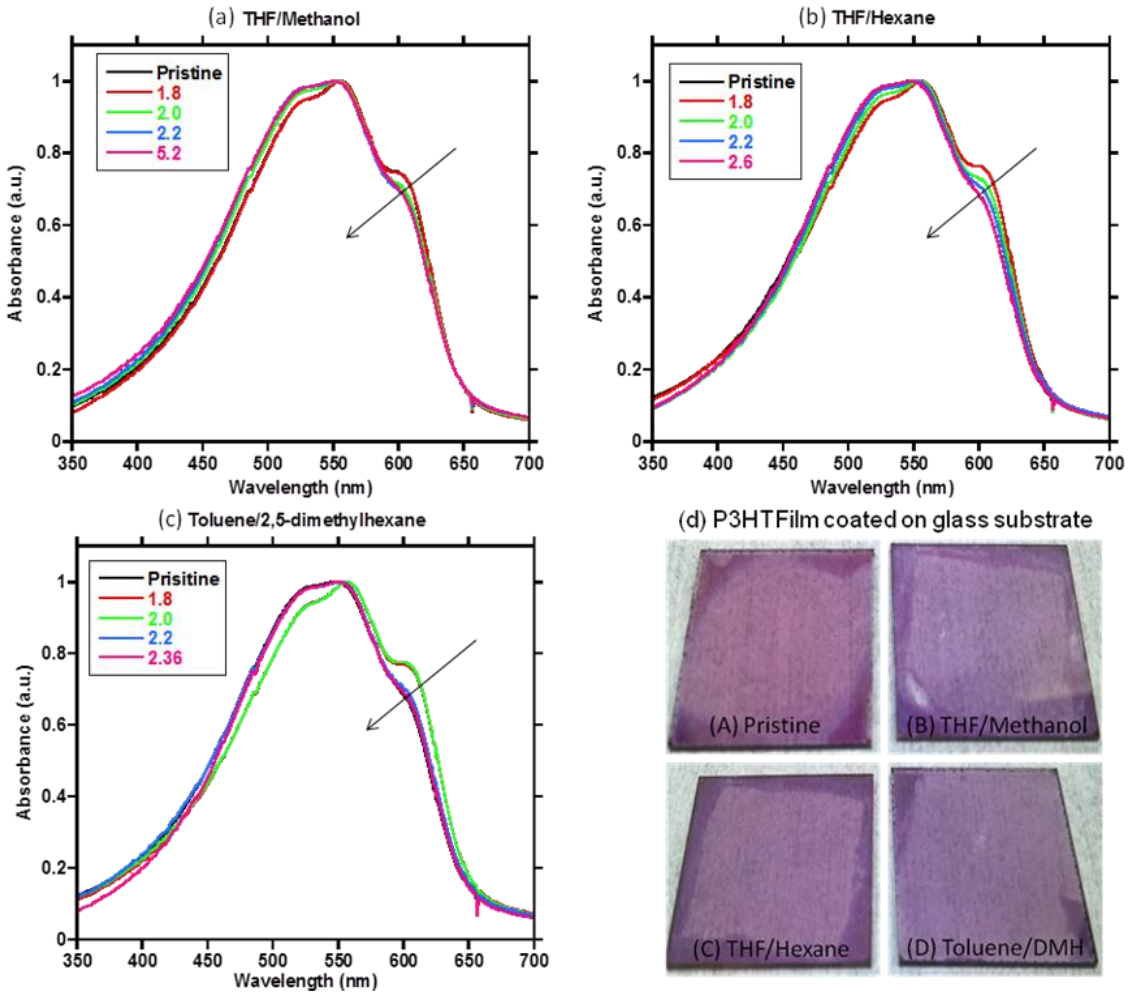


**Figure 28:** UV-vis spectrum change of individual secondary solvents: (a) THF/Methanol, (b) THF/Hexane, (c) Toluene/2,5-dimethylhexane. The changes in UV-vis spectrum with corresponding RED values are shown with arrows. (d) P3HT film images of (A) Pristine, (B) THF/Methanol, (C) THF/Hexane, and (D) Toluene/2,5-dimethylhexane (DMH). The (B)-(D) films are assisted by solvent matched to RED value of 1.8.

According to Figure 28, low boiling polar mixture (THF/Methanol), low boiling non-polar mixture (THF/Hexane), and high boiling non-polar mixture (Toluene/DMH) have decrease in crystalline region as RED values increased. As secondary solvent became more poor, the solvents had less impact on the surface morphology. Although the development of crystalline region of three cases are similar, the difference in mobility may be due to wetting of the secondary solvents. As P3HT is coated on the substrate, the surface become non-polar. Therefore, low boiling polar mixture has poor wetting on a

film and, thus, promote inhomogenity in the film. Polar mixtures have relatively weak affect on the morphology of the film. On the other hand, non-polar mixtures have good wetting on the surface of the film, hence, impacting the film more homogeneously. High boiling non-polar mixtures, resides on the film longer than the low boiling non-polar mixtures. Therefore, Toluene/DMH mixture have more time to induce structured ordering and crystallinity of the film. This eventually leads to superior OFET performances. From Figure 28 (d), we can see subtle color changes from light purple pristine film to slightly darker purple solvent assisted film. Change in molecular structure impacted macroscopic structure of the film, which is visible from the subtle color change.

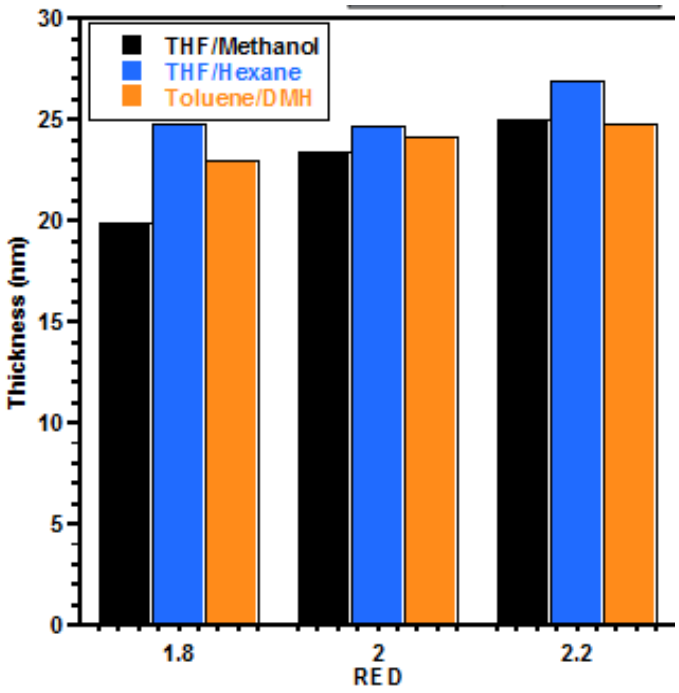


**Figure 29:** Thickness of P3HT films treated with secondary solvents spin-coated on silicon dioxide substrate.

Even though UV-vis spectrum shows a developed red-shift, we observe a decrease in mobility. Therefore another factor other than the ordered aggregation of the film affects the mobility. This can be explained by thickness of the OFET films.[56] Figure 29, shows the thickness of the film at the corresponding RED values. The trend is similar

to the electrical performance data. When more soluble secondary solvents were dropped we had relatively thinner film than the low soluble solvents were dropped. In theory, charge carrier mobility depends on the interface between the polymer and the substrate. Therefore, in thickness is not a factor to induce change in the performance. However, in reality, we speculate there is a bulk charge transport in the entire film, which is influenced by the thickness of the film.

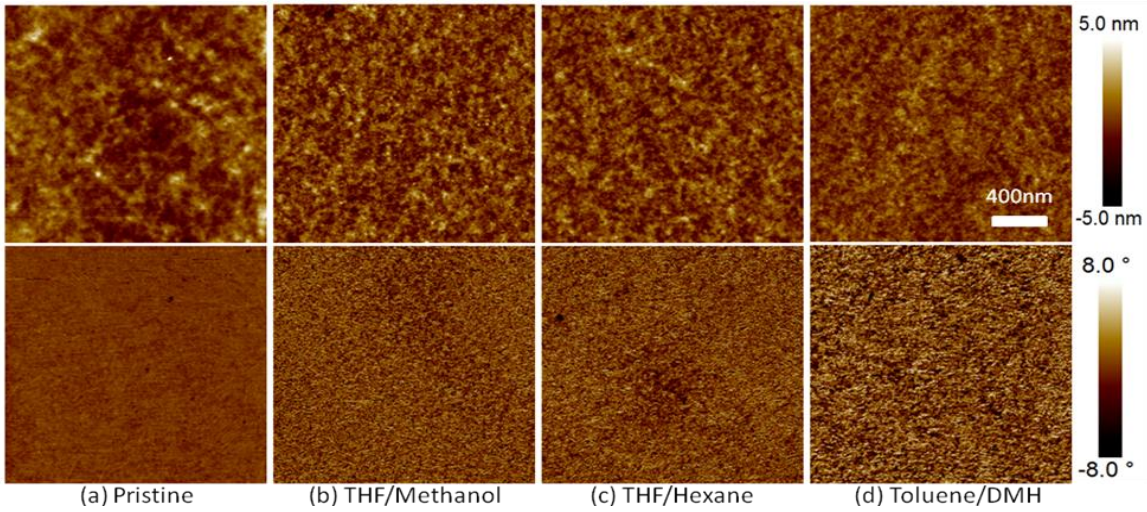


**Figure 30:** Atomic Force Microscopy (AFM) image of representative P3HT films: (a) pristine P3HT, (b) THF/Methanol, (c) THF/Hexane, (d) Toluene/2,5-dimethylhexane (DMH). The upper row shows height images and lower row represents phase images.(b)-(d) are P3HT film images of secondary solvents mixed to match RED value of 2.2.

The AFM image of representative P3HT films that provided highest field-effect mobility is shown in Figure 30. Influenced by molecular structure changes, the difference of macroscopic structure are visible between pristine and solvent assisted films. Evidently, there is a distinctive development of P3HT thin-film structure according to phase regions of Figure (b)-(d). This is not visible in the featureless and amorphous pristine phase region. The rapid evaporation of chloroform during spin-coating process leads to weak molecular packing and amorphous morphology.[42,51] Among the three solvent treated films, high boiling non-polar mixtures have induced good polymer chain packing and evolved high conductive crystalline regions more than low boiling secondary solvents.

## 3.4 Conclusion

In conclusion, solvent assisted technique was systematically studied by varying three parameters: boiling point, polarity, and solubility of the secondary solvents. The mobility of the devices had an increase in trend as RED values increased. This was studied to be the thickness change when secondary solvents were dropped. Thickness of the film had more impact on the mobility than the ordered aggregations. Non-polar solvents had much more impact on the morphology of P3HT thin film, because of better wetting with non-polar P3HT film surface. Therefore, impact of the secondary solvents is provided evenly, increasing homogeneity of the film. Lastly, high boiling point non-polar solvents had developed more crystalline film than low boiling non-polar solvents, The high-boiling non-polar remained on the film surface longer, thus, inducing higher crystallinity and better ordering of the P3HT polymers. One of the problems in solvent-assisted re-annealing technique was the use of high annealing temperature, which is costly to maintain. This study has shown that improvement of OFET performance can be achieved without the need of high annealing temperature. Also benefits of potential application in encapsulation of OFETs and construction of top-gate OFETs can further be achieved with more volatile solvents. In addition, systematic trend has been conducted to help selecting secondary solvents and formulated base study of impact of process parameters modification on OFET film morphology and, thus, electronic properties.

# CHAPTER 4

# CONCLUSIONS

The main focus of the thesis was to improve the OFET performance by investigating the impact of change in process parameters on film morphology and charge transport properties.

In Chapter 2, we successfully showed that the addition of high boiling good solvent (dichlorobenzene) to main solvent (chloroform) have improved the performance of P3HT film OFET. The small addition of dichlorobenzene has developed distinctive nano-fibrous and crystalline structure of P3HT. Both inter- and intra-molecular interaction were improved to form films that support efficient charge transport. The OFET mobility rose due to better packing of the polymer chain and to formulation of high conductive crystalline structure. This method can lead to a low-cost, large-area application due to improvement in processability. By using the method suggested in this chapter, high annealing temperature up to 170℃ is not required. Also SAM layers coated on substrates prior deposition of DCB processed P3HT are unnecessary due to improved wetting on the hydrophilic substrate. Furthermore, high boiling good solvent assisted process can provide alternative method to enhance molecular ordering and control aggregation of π-conjugated semiconductors without the need of post-treatment of polymer.

In Chapter 3, further study of solvent-assisted re-annealing technique was conducted. Solvent-assisted re-annealing technique has potential application in OFET encapsulation and fabrication of top-contact OFET. The novel method for encapsulation will suggest a development of more stable devices. Systematic study of solvent-assisted technique has been done to find solvents that are adequate to anneal in low temperatures and, yet, maintain good performance. Three process parameters: boiling point, polarity,

and solubility were investigated. The high boiling non-polar solvents with relatively high RED values promoted ordered molecular packing and hence, formulated crystalline structure, which improved device performance. This method provides general route to improve OFET performance and suggest low-cost device fabrication process.

In conclusion, process parameters are significant factors to find further improvement of device performance of OFET. By controlling process parameters we can further understand the formulation of polymer film morphology and electronic properties that can be implied to various applications such as light emitting diodes and organic photovoltaic cells.

## 4.1 Future Work

The above thesis provides methods to control morphology of the film to enhance film performance. The research can be further by integrating stability into this morphological change. Without sustaining stability, high performing devices are not much of a use. Therefore, my further interest is enhancing stability of the device by mixing an organic semi-conductive polymer and insulating polymer, such as polystyrene, together. We expect insulating polymer will protect the semi-conductive polymer from the oxygen. The addition of polystyrene to P3HT solution is expected to maintain good mobility and improve the stability of the device.

In addition, instead of varying a volatility of P3HT solution by introducing multiple solvents, we can control the operating conditions such as temperature and pressure to adjust vapor pressure of single-solvent P3HT solution. This mechanical adjustment will introduce smaller variables, such as solvent-solvent interaction of mixtures, to the system. By controlling vapor pressure, we can also provide a simple alternatives to control the morphology of the semi-conductive film.

# REFERENCES


[1] G. Gustafsson, Y. Cao, G.M. Treacy, F. Klavetter, N. Colarneri, A.J.Heeger. Flexible Light-Emitting-Diodes Made from Soluble Conducting Polymers. Nature 357: 477-479, 1992

[2] J.A. Rogers, Z. Bao, K. Baldwin, A. Dodabalapur, B. Crone, V.R. Raju, V. Kuck, H. Katz, K. Amundson, and J. Ewing. Paper-like electronic displays: Large-area rubber-stamped plastic sheets of electronics and microencapsulated electrophoretic inks. P. Natl. Acad. Sci., 98(9):4835, 2001

[3] ScienceDaily Fraunhofer ISE 2008.URL:http://www.sciencedaily.com/releases/2008/02/080206154631.htm [Online; accessed Nov 2013].

[4] Plastic Electronics, Sara Ver-Bruggen, 2011 URL: https://pira.revolutiondata-cms.com/uploads/public/images/Plastic%20Electronics%20Magazine/Consumer%20Electronics/Analysis/COPE%20OFETs%20250.jpg [Online; accessed Nov 2013]

[5] TechsFuture.com, Ayush Parmar, 2013 URL: techsfuture.com/flexible e paperconcept.html [Online; accessed Nov 2013]

[6] Wikipedia, Heiko Kempa 2008 URL: http://en.wikipedia.org/wiki/File:Complementary Technologies.png, [Online; accessed Nov 2013]

[7] R.G. Kepler. Charge carrier production and mobility in anthracene crystals. Phys. Rev., 119(4):1226, 1960

[8] C. K. Chiang, C. R. Fincher, Y. W. Park, A. J. Heeger, H. Shirakawa, E. J., Louis, S. C. Gau, and Alan G. MacDiarmid. Electrical conductivity in doped polyacetylene. Phys. Rev. Lett., 39(17):1098, 1977.

[9] A. Moliton, and R.C. Hiorns. The origin and development of (plastic) organic electronics. Polym. Int., 61: 337–341. doi: 10.1002/pi.4173 (2012)

[10] The University of Western Ontario, Brain Pagenkopf,URL: http://instruct.uwo.ca/chemistry/373f/Nifty%20Stuff/ethylene.htm, [Online; accessed Nov 2013]

[11] J. Bredas, J. Cornil, and A.J. Heeger. The exciton binding energy in luminescent conjugated polymers. Adv. Mater., 8(5):447-452, 1996.

[12] W. R. Salaneck, R. H. Friend, and J. L. Bredas. Electronic structure of conju- gated polymers: consequences of electron-lattice coupling. Phys. Rep., 319(6): 231-251, 1999.

[13] Z. Bao and J.J. Locklin. Organic Field-Effect Transistors, volume 128. CRC, 2007.

[14] Principles of Semiconductor Devices, Bart Van Zeghbroeck, 2011 URL: http://ecee.colorado.edu/~bart/book/book/chapter2/ch2_7.htm [Online; accessed Nov 2013]

[15] N.S. Hush. Adiabatic rate processes at electrodes. i. energy charge relationships. J. Chem. Phys., 28:962, 1958.

[16] R.A. Marcus. On the theory of oxidation reduction reactions involving electron transfer. i. J. Chem. Phys., 24:966, 1956.

[17] J. M. Shaw and P. F. Seidler. Organic electronics: Introduction. IBM J. Res. Dev., 45(1):3-9, 2001.

[18] S.F.Nelson, Y.Y. Lin, D.J. Gundlach, and T.N. Jackson, Appl.Phys. Lett. 1998, 72, 1854.

[19] I. McCulloch. Thin films: Rolling out organic electronics. Nat. Mater., 4(8): 583-584, 2005. 10.1038/nmat1443.

[20] Frommer, Jane E. (1986). "Conducting polymer solutions". Accounts of Chemical Research 19: 2.

[21] Elsenbaumer, R.; Jen, K.; Oboodi, R. (1986). "Processible and environmentally stable conducting polymers☆". Synthetic Metals 15 (2–3): 169

[22] Z. Bao, A. Dodabalapur, and A.J. Lovinger. Soluble and processable regioregular poly(3-hexylthiophene) for thin film field-effect transistor applications with high mobility. Appl. Phys. Lett., 69(26):4108-4110, 1996.

[23] Wikipedia, Polythiophene, 2013 URL: http://commons.wikimedia.org/wiki/File:Polythiophene_structure.svg [Online; accessed Nov 2013]

[24] Sigma Aldrich, P3HT and Pentacene URL: http://www.sigmaaldrich.com/catalog/product/aldrich/p1802?lang=en&region=US [Online; accessed Nov 2013]

[25] Aiyar, A. (2012) Understanding the Impact of Polymer Self-organization On The Microstructure and Charge Transport In Poly(3-hexylthiophene), (Doctoral dissertation, Georgia Institute of Technology, Atlanta, GA). Retrieved from https://smartech.gatech.edu/handle/1853/43574

[26] Koezuka, H.; Tsumura, A.; Ando, T. (1987). "Field-effect transistor with polythiophene thin film". Synthetic Metals 18: 699–704.

[27] Kline, R.J., McGehee, M.D., Kadnikova, E.N., Liu, J. and Fréchet, J.M.J. (2003), Controlling the Field-Effect Mobility of Regioregular Polythiophene by Changing the Molecular Weight. Adv. Mater., 15: 1519–1522. doi: 10.1002/adma.200305275

[28] Antonio Facchetti. Semiconductors for organic transistors. Mater. Today, 10 (3):28-37, 2007.

[29] G. Horowitz, “Organic thin film transistors: From theory to real devices,” J. Mater. Res., vol. 19, pp. 1946–1962, 2004.

[30] C. D. Dimitrakopoulos and D. J. Mascaro, “Organic thin-film transistors, a review of recent advances,” IBM J. Res. Dev., vol. 45, pp. 11–27, 2001.

[31] Hamadani, Behrang H. (2007) Electronic Charge Injection and Transport in Organic Field-Effect Transistors (Doctoral dissertation, Rice University, Houston, Texas). Retrieved from http://www.ruf.rice.edu/~natelson/theses/

[32] Newman, C.R., Daniel Frisbie, C., da Silva Filho, D.A., Bredas, J.-L., Ewbank, P.C., and Mann, K.R., “Introduction to organic thin film transistors and design of n-channel organic semiconductors” American Chem,16(23) 4436-4451, 2004,

[33] Chang, M., Choi, D., Fu, B., Reichmanis, E. “Solvent based hydrogen bonding: Impact on poly(3-hexylthiophene) nanoscale morphology and charge transport characteristics” ACS Nano, 2013, 7 (6), pp 5402–5413, 2013.

[34] Aiyar, A. R.; Hong, J. I.; Reichmanis, E. Regioregularity and Intrachain Ordering: Impact on the Nanostructure and Charge Transport in Two-Dimensional Assemblies of Poly-(3-hexylthiophene). Chem. Mater. 2012, 24, 2845–2853.

[35] Kline, R. J.; McGehee, M. D.; Kadnikova, E. N.; Liu, J. S.; Frechet, J. M. J. Controlling the Field-Effect Mobility of Regioregular Polythiophene by Changing the Molecular Weight. Adv. Mater. 2003, 15, 1519–1522.

[36] Zhang, R.; Li, B.; Iovu, M. C.; Jeffries-EL, M.; Sauve, G.; Cooper, J.; Jia, S. J.; Tristram-Nagle, S.; Smilgies, D. M.; Lambeth, D. N.; et al. Nanostructure Dependence of Field-Effect Mobility in Regioregular Poly(3-hexylthiophene)Thin Film Field Effect Transistors. J. Am. Chem. Soc. 2006, 128, 3480–3481

[37] H. Yang, T. J. Shin, L. Yang, K. Cho, C. Y. Ryu, and Z. Bao. Effect of mesoscale crystalline structure on the field-effect mobility of regioregular poly(3-hexyl thiophene) in thin-film transistors. Adv. Funct. Mater., 15(4):671-676, 2005.

[38] Moule, A. J.; Meerholz, K. Controlling Morphology inPolymer-Fullerene Mixtures. Adv. Mater. 2008, 20, 240–245.

[39] Kiriy, N.; Jahne, E.; Adler, H. J.; Schneider, M.; Kiriy, A.; Gorodyska, G.; Minko, S.; Jehnichen, D.; Simon, P.; Fokin, A. A.; et al. One-Dimensional Aggregation of Regioregular Polyalkylthiophenes. Nano Lett. 2003, 3, 707–712.

[40] Li, L. G.; Lu, G. H.; Yang, X. N. Improving Performance of Polymer Photovoltaic Devices Using an Annealing-Free Approach via Construction of Ordered Aggregates in Solution. J. Mater. Chem. 2008, 18, 1984–1990.

[41] Park, Y. D.; Lee, H. S.; Choi, Y. J.; Kwak, D.; Cho, J. H.; Lee, S.; Cho, K. Solubility-Induced Ordered Polythiophene Precursors for High-Performance Organic Thin-Film Transistors. Adv. Funct. Mater. 2009, 19, 1200–1206.

[42] Chang, J. F.; Sun, B. Q.; Breiby, D. W.; Nielsen, M. M.; Solling, T. I.; Giles, M.; McCulloch, I.; Sirringhaus, H. Enhanced Mobility of Poly(3-hexylthiophene) Transistors by Spin-Coating from High-Boiling-Point Solvents. Chem. Mater. 2004, 16, 4772–4776.

[43] Dimitri Janssen, Randy De Palma, Stijn Verlaak, Paul Heremans, Wim Dehaen Static solvent contact angle measurements, surface free energy and wettability determination of various self-assembled monolayers on silicon dioxide Thin Solid Films, Volume 515, Issue 4, 5 December 2006, Pages 1433–1438

[44] Jia, H. P.; Gowrisanker, S.; Pant, G. K.; Wallace, R. M.; Gnade, B. E. Effect of Poly (3-hexylthiophene) Film Thickness on Organic Thin Film Transistor Properties. J. Vac. Sci. Technol.,A 2006, 24, 1228–1232.

[45] Brown, P. J.; Thomas, D. S.; Kohler, A.; Wilson, J. S.; Kim, J. S.; Ramsdale, C. M.; Sirringhaus, H.; Friend, R. H. Effect of Interchain Interactions on the Absorption and Emission of Poly(3-hexylthiophene). Phys. Rev. B 2003, 67, 064203.

[46] J. Clark, J. F. Chang, F. C. Spano, R. H. Friend, C. Silva, "Determining exciton bandwidth and film microstructure in polythiophene films using linear absorption spectroscopy" Appl. Phys. Lett. 2009, 94, 163306.

[47] Mcculloch, I.; Heeney, M.; Bailey, C.; Genevicius, K.; I, M.; Shkunov, M.; Sparrowe, D.; Tierney, S.; Wagner, R.; Zhang, W. M.; et al. Liquid-Crystalline Semiconducting Polymers with High Charge-Carrier Mobility. Nat. Mater. 2006, 5, 328–333.

[48] Nagarjuna, G; Baghgar, M.; Labastide, J. A.; Algaier, D. D.; Barnes, M. D.; Venkataraman, D. "Tuning Aggregation of Poly(3-hexylthiophene) Within Nanoparticles," ACS Nano, 2012, 6, 10750-10758.

[49] Prosa, T. J.; Winokur, M. J.; Moulton, J.; Smith, P.; Heeger, A. J. X-Ray Structural Studies of Poly(3-alkylthiophenes): An Example of an Inverse Comb. Macromolecules 1992, 25,4364–4372.

[50] Aiyar, A. R.; Hong, J. I.; Nambiar, R.; Collard, D. M.; Reichmanis, E. Tunable Crystallinity in Regioregular Poly-(3-Hexylthiophene) Thin Films and Its Impact on Field Effect Mobility. Adv. Funct. Mater. 2011, 21, 2652–2659.

[51] Yang, H. H.; LeFevre, S. W.; Ryu, C. Y.; Bao, Z. N. Solubility-Driven Thin Film Structures of Regioregular Poly(3-hexylthiophene) Using Volatile Solvents. Appl. Phys. Lett. 2007,90, 172116.

[52] I. McCulloch, M. Heeney, C. Bailey, K. Genevicius, I. MacDonald,M. Shkunov, D. Sparrowe, S. Tierney, R. Wagner, W. Zhang, M. L. Chabinyc, R. J. Kline, M. D.

McGehee, M. F. Toney,, “Liquid-crystalline semiconducting polymers with high charge-carrier mobility.” Nat. Mater. 2006, 5, 328.

[53] H. Ebata, T. Izawa, E. Miyazaki, K. Takimiya, M. Ikeda, H. Kuwabara, T. Yui, J. Am., “Very High Mobility in Solution-Processed Organic Thin-Film Transistors of Highly Ordered [1]Benzothieno[3,2-b]benzothiophene Derivatives” Chem. Soc. 2007, 129, 15732.

[54] B. S. Ong, Y. L. Wu, P. Liu, S. Gardner, Adv. Mater. 2005, 17, 1141

[55] Di, C.-a., Lu, K., Zhang, L., Liu, Y., Guo, Y., Sun, X., Wen, Y., Yu, G. and Zhu, D. (2010), Solvent-Assisted Re-annealing of Polymer Films for Solution-Processable Organic Field-Effect Transistors. Adv. Mater., 22: 1273–1277.

[56] Blaise A. Pinaud, Peter C. K. Vesborg, and Thomas F. Jaramillo (2012), Effect of Film Morphology and Thickness on Charge Transport in Ta3N5/Ta Photoanodes for Solar Water Splitting *The Journal of Physical Chemistry C 116* (30), 15918-15924